Geological Society of America Bulletin

Late Pleistocene–Holocene retreat of the West Antarctic Ice-Sheet system in the Ross Sea: Part 1 —Geophysical results

Stephanie Ship, John Anderson and Eugene Domack

Geological Society of America Bulletin 1999;111, no. 10;1486-1516
doi: 10.1130/0016-7606(1999)111<1486:LPHROT>2.3.CO;2

Late Pleistocene–Holocene retreat of the West Antarctic Ice-Sheet system in the Ross Sea: Part 1—Geophysical results

Stephanie Shipp* } *Department of Geology and Geophysics, Rice University, P.O. Box 1892, 6100 South Main, Houston, Texas 77005*
John Anderson }

Eugene Domack *Department of Geology, Hamilton College, Clinton, New York 13323*

ABSTRACT

In the 1994, 1995, and 1998 austral field seasons, geophysical research efforts in the Ross Sea focused on acquiring a high-resolution database designed to permit (1) reconstruction of the maximum extent and configuration of the ice sheet during the Last Glacial Maximum (i.e., oxygen isotope stage 2); (2) reconstruction of conditions at the base of the ice sheet; and (3) assessment of the relative retreat history of the ice sheet following the Last Glacial Maximum.

Five seismic facies are distinguished on the basis of external geometry, relationships among features, bounding surface amplitude, intensity of internal acoustic signature, and geometry of internal reflectors. Seismic facies 1 is a transparent draping unit correlated to diatomaceous mud, interpreted as being deposited under open-marine conditions. Seismic facies 2 and 3 are comprised of units displaying subdued massive internal signatures with smooth lower bounding surfaces and hummocky upper surfaces characterized by glacial lineations. These units are interpreted to be grounding-zone proximal deposits overridden by the expanded ice sheet. Seismic facies 2 may be a deforming-till unit. Seismic facies 4a is characterized by an internally massive to chaotic signature, an erosional, often flat, lower surface, and a hummocky upper surface displaying glacial lineations. This unit is interpreted to be till and is divided into deposits associated with the most recent glacial expansion (4a) and with an earlier (pre–Last Glacial Maximum) expansion (4b). Seismic facies 5 is an acoustically laminated, ponded, and draping deposit interpreted to contain proglacial and sub–ice-shelf materials deposited continuously since the last interglacial period. The associations of these units provide context for the interpretation of the ice-edge maximum position, conditions at the base of the ice sheet, and the relative retreat history of the region.

There is compelling evidence for a much-expanded ice sheet in the Ross Sea during the Last Glacial Maximum. In the western Ross Sea, the maximum grounding position is marked by an isolated grounding-zone wedge, and placed in the vicinity of Coulman Island, approximately 150 km from the continental-shelf edge. In the central Ross Sea, the maximum grounding position is close to the continental-shelf break, based primarily on the presence of an extensive 60-m-thick sheet-like deposit with a fluted upper surface.

Streaming ice may have occupied bathymetric lows on the continental shelf, as suggested by (1) the configuration of bathymetry; (2) the presence of glacially eroded troughs; (3) the concentration of sediment (interpreted to be deforming till) within the middle to outer shelf reaches of the troughs; and (4) the fluted nature of the upper surface. Absolute rates of streaming ice flow relative to inter–ice-stream areas are not implied.

The western Ross Sea continental-shelf deposits record the retreat history of ice derived predominantly from the East Antarctic Ice Sheet and glaciers of the Transantarctic Mountains. Ice flow on the continental shelf is interpreted to have remained fixed in position, restricted by the walls of the troughs. On the inner shelf of the western Ross Sea, the ice flowed over and eroded lithified sedimentary strata. Slower-moving ice occupied flat-topped banks. A single grounding-zone wedge occurs on the western Ross Sea central shelf; no substantial deposits are observed on the inner continental shelf. This lack of grounding-zone features reflects a restricted sediment supply and a relatively steady, rapid retreat of the ice sheet. During retreat, ice flow acted independently in each major trough and on the bank tops. Ice retreated from Victoria Land Basin–Drygalski Trough before it retreated from JOIDES Basin. Ice remained on the bank tops, shedding material into the abandoned troughs.

Grounded ice in the central Ross Sea was derived predominantly from an expanded West Antarctic Ice Sheet. The ice sheet remained grounded on the continental-shelf edge after retreat of ice from the western Ross Sea. Expanded ice eroded the inner shelf and deposited sheets of till on the central and outer shelf. Ice-stream drainage shifted laterally, as recorded by rounded, laterally accreting ridges that separate bathymetric troughs. The central Ross Sea is the repository for larger volumes of sediment, derived from ice flow across basins of relatively thick, unlithified sedimentary deposits. Two till sheets mark grounding-zone positions in the central Ross Sea, reflecting the higher sediment supply and a stepped deglaciation. Ice remained grounded on the Pennell Bank to the west; a series of moraines marks the retreat of ice across the bank.

Mega-scale glacial lineations and other streamlined, subglacial geomorphic features occur across the continental shelf, primarily within the troughs. The lineations substantiate the maximum reconstruction and support the interpretation of a deforming substrate beneath the outer reaches of the expanded ice sheet. This deforming substrate may have contributed to the onset of deglaciation. Features associated with meltwater are rare or absent, suggesting that basal meltwater played a minor role in retreat of the ice sheet.

INTRODUCTION

Many key questions about late Quaternary geology revolve around the expansion and contraction of the Antarctic Ice Sheet. Were ice-sheet fluctuations in phase with the Northern Hemisphere ice sheets? Did the East and

*E-mail: shippst@ruf.rice.edu.

GSA Bulletin; October 1999; v. 111; no. 10; p. 1486–1516; 16 figures; 2 tables.

West Antarctic Ice Sheets expand and contract in concert? What, and when, was the contribution of Antarctic ice to global sea level during the past 18 k.y.? Does the West Antarctic Ice Sheet have a history of catastrophic collapse? How does the geologic setting of the continental shelf (e.g., bed topography, sediment cover, and character) influence the behavior of the ice sheet and its potential to collapse? Resolving these questions requires documentation of the maximum extent of the ice sheet during the Last Glacial Maximum (LGM), characterization of deposits and geomorphic features that existed under the expanded ice sheet, and establishment of the history of ice-sheet retreat.

The questions of maximum limits of ice grounding and rates of retreat from the Ross Sea are central to the debate on possible future behavior of the West Antarctic Ice Sheet and predictions about future sea-level change (Bentley, 1997; Bindschadler, 1997a; Bindschadler et al., 1998). Collapse of marine-based ice sheets has been proposed by researchers working in the Northern Hemisphere (Heinrich, 1988; Andrews and Tedesco, 1992; Bond et al., 1992). Anderson and Thomas (1991) argued that periodic collapse of marine ice sheets is the most likely mechanism to explain rapid eustatic rises during the past 18 k.y. They stressed that, although the magnitude of these collapse events (<2 m) often is too small to be observed as rises on the global sea-level curve (e.g., Fairbanks, 1989), the rises occurred so rapidly that they caused significant, and observable, shifts in coastal systems (Thomas and Anderson, 1994). Similar small increases in sea level in the future would have a large impact on human populations located near the present shoreline.

If pulses of rapid ice-sheet retreat occurred since the LGM, similar rapid retreat of the ice mass could occur in the future. The West Antarctic Ice Sheet is the sole extant marine-based ice sheet; disintegration of the entire West Antarctic Ice Sheet would result in a eustatic sea-level rise of approximately 6 m (Denton et al., 1991). Considerable speculation has focused on the stability of the marine-based West Antarctic Ice Sheet (e.g., Hollin, 1962; Hughes, 1973, 1977, 1987; Thomas and Bentley, 1978; Blankenship et al., 1986; Alley et al., 1986, 1987a; Denton et al., 1991; Lingle et al., 1991; MacAyeal, 1992; Bentley, 1997; Bindschadler, 1997a; Bindschadler et al., 1998; Oppenheimer, 1998). Recent investigations assessed the mechanisms that may result in instability of the West Antarctic Ice Sheet, such as a deforming substrate (e.g., Alley et al., 1986, 1987a; MacAyeal, 1992), a rise in sea level (e.g., Hollin, 1962; Thomas and Bentley, 1978; Lingle and Clark, 1979; Hughes, 1987; Lingle et al., 1991), or undermelting of an ice shelf by relatively warm water masses flowing onto the continental shelf (e.g., Potter and Paren, 1985; Jacobs et al., 1996; Jenkens et al., 1996).

Approximately 25% of the Antarctic Ice Sheet discharges into the Ross Sea, including contributions from the West and East Antarctic Ice Sheets, making this region a valuable focus for monitoring past ice-sheet activity (Denton et al., 1989; Fig. 1). This study was designed to provide constraints on the extent and configuration of the ice sheets in the Ross Sea during the LGM, their relative retreat histories, conditions at their bases, and the stratigraphic intervals related to retreat. An understanding of the extent and behavior of the ice sheets during the LGM will allow partial assessment of the links between deglaciation and internal and external environmental influences, and will aid in the development of models for future activity of the ice sheets.

INVESTIGATION SETTING

The study region is bounded on the west by the Transantarctic Mountains of the Victoria Land coast, to the east by the eastern Ross Sea, to the south by the Ross Ice Shelf edge and to the north by the continental-shelf break (Figs. 1 and 2). Continental-shelf depths range from less than 250 m to greater than 1200 m and average greater than 500 m (Barnes and Lien, 1988; Davey, 1994). A series of northeast-southwest–trending ridges and troughs dominates the bathymetry. The troughs are foredeepened; the inner shelf is deeper than the outer shelf because of repeated periods of glacial erosion during which material was removed from the inner shelf and transported to the outer shelf (Johnson et al., 1982; ten Brink et al., 1995).

PREVIOUS INVESTIGATIONS

A nearly century-long debate over the size of the ice sheet in the Ross Sea region during the LGM has resulted in several models for ice expansion (e.g., Debenham, 1921; Hughes, 1977; Drewry 1979; Stuiver et al., 1981; Denton et al., 1989, 1991; Kellogg et al., 1996). These models differ in the extent and thickness of the marine ice sheet and ice shelf. The majority of these reconstructions do not incorporate substantial marine geological evidence from the Ross Sea continental shelf, primarily because it was not available. Hughes (1977) put forth the suggestion that the northeast-southwest–trending troughs that characterize the sea floor reflect extension of West Antarctic Ice Sheet ice streams A through F across the continental shelf during glacial advances (Fig. 1), but little evidence beyond the bathymetry was available to constrain the grounding line. Combining glaciological and geological data, Drewry (1979) proposed a LGM reconstruction in which an ice shelf covered most of the Ross Sea. Drewry's (1979) model hypothesized minimal advance of the present grounding line and grounding by the ice shelf only on the shallow banks of the continental shelf. The numerical Climate Long-range Investigation Mapping and Planning (CLIMAP) models of Stuiver et al. (1981) presented maximum and minimum configurations of grounded ice in the Ross Sea during the LGM. The maximum reconstruction is based on geologic data and calls for extensive grounding. The minimum model is governed by glaciological data and depicts little change in ice extent. Denton et al. (1989) refined Stuiver et al.'s (1981) models for the Ross Sea region on the basis of additional geological and glaciological evidence. They proposed a minimum model in which ice streams were active and grounded ice advanced across the banks of the western Ross Sea but did not ground on the outer shelf within the troughs. Central Ross Sea was devoid of grounded ice but was covered by an ice shelf. In Denton et al.'s (1989) maximum model, ice streams were not active, thus ice was able to accumulate and extend to the continental-shelf edge. The outer shelf of the western Ross Sea remained ice free. Kellogg et al. (1996) developed a series of flow-line reconstructions for retreat stages of grounded ice from the western Ross Sea, based primarily on geologic observations from the McMurdo Ice Shelf region and valley glaciers of the Transantarctic Mountains. The models emphasize the contribution by the East Antarctic Ice Sheet to this sector of the Ross Sea. In their maximum reconstruction, ice was grounded to the continental-shelf edge, although the authors indicate that this configuration could have occurred during a previous glaciation. The models suggest that ice remained grounded on the banks of the Ross Sea; ice retreated initially from Victoria Land Basin, followed by retreat from Joint Oceanographic Institutions for Deep Earth Sampling (JOIDES) Basin (Fig. 2).

Initial marine geophysical investigations in the Ross Sea identified the presence of an extensive unconformity capped by an acoustically massive unit (e.g., Houtz and Davey, 1973; Hayes and Davey, 1975; Karl et al., 1987). The unconformity was interpreted to be created by glacial erosion, with till comprising the overlying deposits. Later work demonstrated that several glacial-erosional unconformities, capped by thin acoustically massive units, characterize the strata of the region above and below the originally identified unconformity (e.g., Alonso et al., 1992; Anderson and Bartek, 1992). Based on sedimentologic and higher-resolution seismic (sparker) data in the western Ross Sea, Reid (1989) placed the LGM grounding line slightly north of Coulman Island. Subsequent seismic inves-

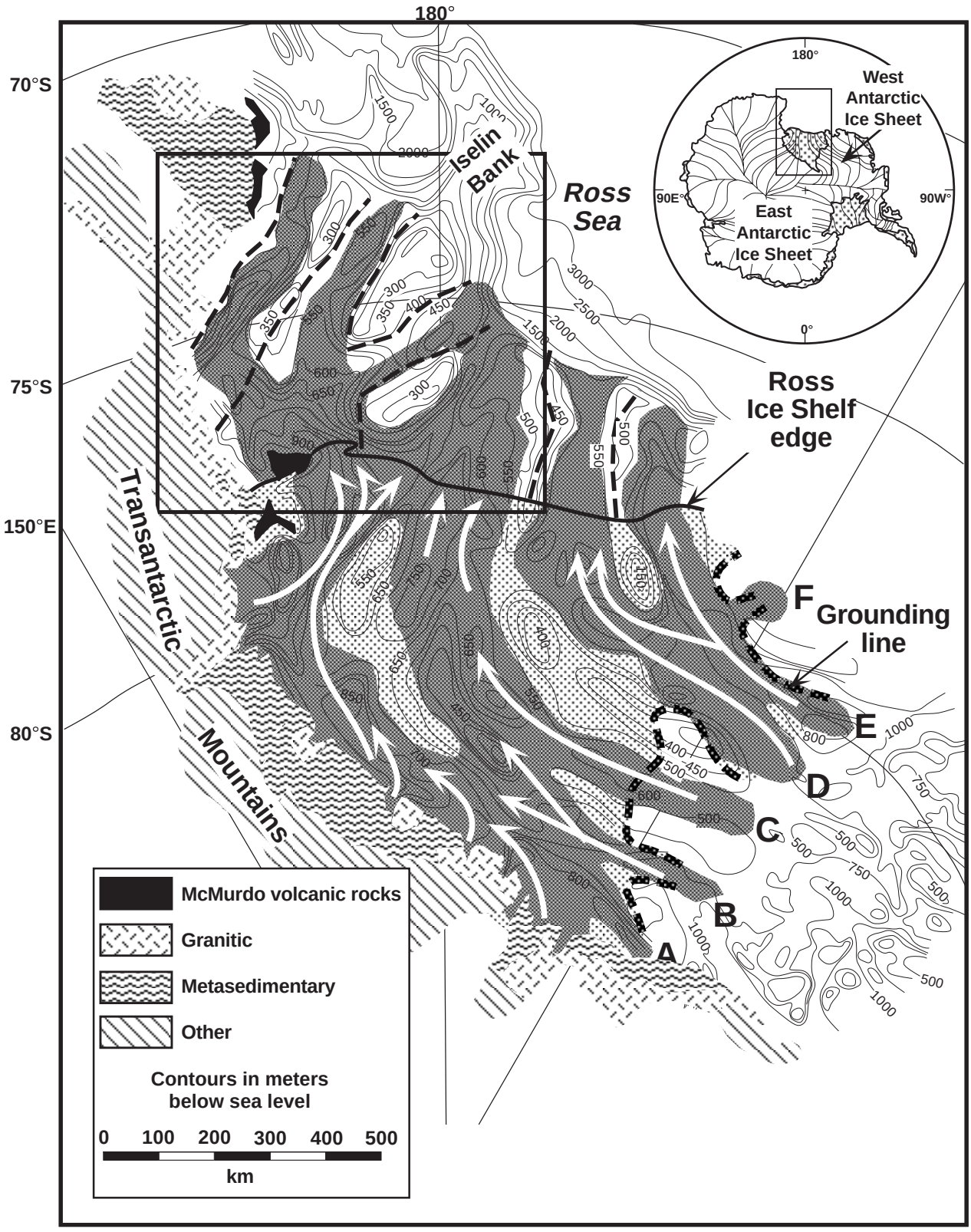

Figure 1. Bathymetric and subglacial topographic map (from Bentley and Jezek, 1981). Lightly stippled region indicates the Ross Ice Shelf. A heavy dashed line marks the present grounding line. Extension of paleo-ice streams shown with dark stipple on the continental shelf (from Stuiver et al., 1981). Letters indicate the individual ice streams under the present ice-sheet configuration. Petrographic regions of Victoria Land from Reid (1989). Dashed lines on the continental shelf mark the individual petrographic provinces within the troughs (Reid, 1989; Anderson et al., 1992; Jahns, 1994). Box indicates the area of this investigation. Inset map shows location of the Ross Sea and drainage from the Antarctic Ice Sheet (AIS).

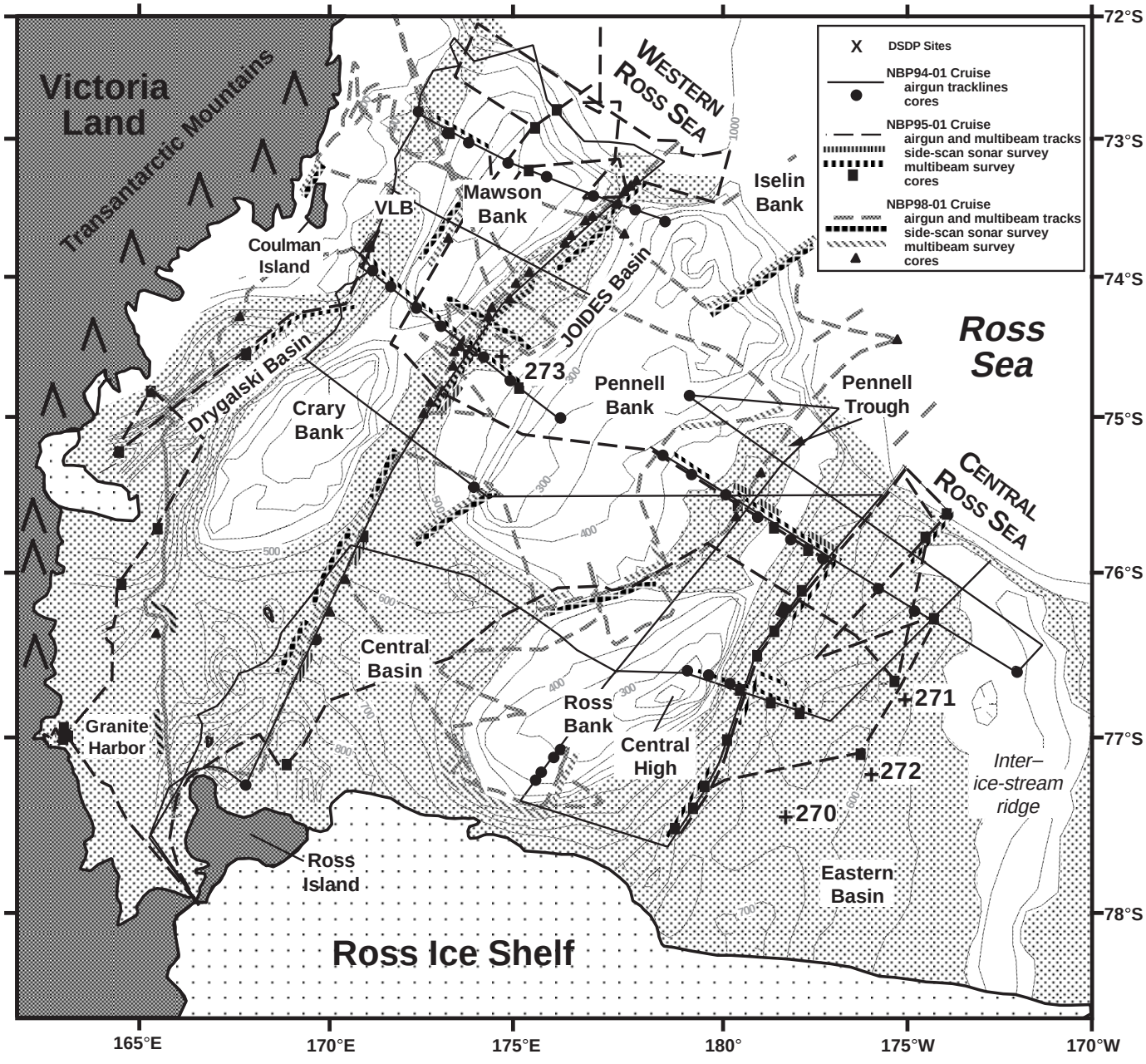

Figure 2. Geological and geophysical data collected during 1994, 1995, and 1998 RV/IB *Nathaniel B. Palmer* cruises. Also shown are bathymetry (contours in meters) and geography, and the location of Deep Sea Drilling Project Sites 270–273. VLB—Victoria Land Basin. Depths greater than 500 m marked by light gray stipple.

tigations identified the presence of an additional grounding-line feature, possibly pre–LGM, at the shelf edge of the western Ross Sea (Anderson et al., 1992). The positioning of the "Coulman Island grounding zone" in the western Ross Sea has been the subject of several investigations (e.g., Domack et al., 1995a, 1995b, 1999a [companion paper in this *Bulletin* issue]; Licht, 1995; Licht et al., 1995, 1996, 1999; Hilfinger et al., 1995; Shipp et al., this study). Licht et al. (1999) placed the LGM grounding line 80 km south of Coulman Island in Victoria Land Basin, and 240 km south of the continental-shelf edge in JOIDES Basin, based on the presence of stratified, foraminifer-rich diamicton, intact radiocarbon stratigraphies, and the presence of tephra layers on the outer continental shelf (see Domack et al., 1999a). This investigation places the JOIDES Basin grounding line approximately 90 km farther north, 150 km from the continental-shelf edge, and tentatively places the Victoria Land Basin grounding line just north of Coulman Island, approximately 130 km from the continental-shelf edge. These interpretations are based on seismic character and glacial-geomorphic features (this study), and on detailed lithofacies, facies relationships, and radiocarbon stratigraphies (Domack et al., 1999a).

TABLE 1. SEISMIC DATABASE

Data type	50 in^3 airgun*	Subbottom profiler	Deep-tow CHIRP	Swath bathymetry	Side-scan sonar
1994 (km)	4100	4100	0	0	0
1995 (km)	3041	8052	0	8052	0
1998 (km)	78	5217	876	5217	876
Total (km)	7219	17 369	876	13 269	876
Ship speed (knots)	4–6	varied (<12 knots)	2–5	varied (<12 knots)	2–5
Best observed resolution (m)	10 vertical	2 vertical	1 vertical	20 (horizontal)	5 (horizontal)
Frequency	80–120 Hz	3.5 kHz (predominant)		12 kHz	
System	Seismic Systems, Inc. generator-injector airgun®; Innovative Transducers® channel streamer; solid-core single-channel streamer; Analog EPC® thermal plotters; Digital: Elics® seismic acquisition software	1994 1995 and 1998: Bathy 2000® deep/shallow water echo-sounder system	DataSonics®	Hull-mounted SeaBeam 2100® swath bathymetry system (120 beams)	DataSonics®
Processing	None	None	None	Removed anomalous records, outer 10 beams, anomalous spikes; Applied corrected sound-velocity profile; Gridded and displayed as shaded relief map with gray-scale continuous fill	None
Archiving	Rice University	Hamilton College	Rice University	Rice University	Rice University

*819 cm^3.

METHODS

Earlier geophysical investigations assisted in identification of the scale of features associated with the LGM, and therefore permitted the selection of equipment to image the features and facies of interest in this study. The geophysical database for this study includes 50 in^3 (819.5 cm^3) airgun seismic profiles, 3.5 kHz (CHIRP) transects, swath bathymetry data, and deep-tow side-scan and CHIRP-sonar data (Fig. 2). Geologic data include piston, kasten, and gravity (trigger) cores and Smith-McIntyre grab samples (Domack et al., 1999a). Seismic acquisition and processing parameters are provided in Table 1. Resolution of the databases varies, but correlation among data types is possible. The lowest resolution data are the 50 in^3 airgun data. These data permit identification of major erosional surfaces and characterization of subsurface strata and larger features. The 50 in^3 airgun data have a bubble-pulse ranging from 10 to 25 m; the thinnest surface layer resolvable is ~10 m. The higher-resolution 3.5 kHz and CHIRP-sonar data permit characterization of the upper tens of meters of the strata, but little penetration into the substrate. Although the thinnest observed layer is 1 m, these data can be correlated directly with the piston (typically less than 3 m) and kasten cores (2 m), and in some instances, with the 50 in^3 airgun data. This allows delineation of sediment thickness and facies relationships within the surface layer. The core data are invaluable for determining the deglacial stratigraphy and establishing a chronostratigraphic context (see Domack et al., 1999a). Swath bathymetry data allow characterization of sea-floor features, while side-scan sonar data record sea-floor features at a finer scale (Table 1).

Seismic stratigraphic units were determined on the basis of the external geometry and relationships among features, bounding surface (reflection) amplitude, intensity of internal acoustic signature, and geometry of internal reflectors. Similar methods have been employed by other investigators for comparable databases in glaciated regions (e.g., King and Fader, 1986; Belknap and Shipp, 1991; King et al., 1991). Thickness and depth estimates are based on conversions of traveltime to depth that assume a velocity of 2000 m/s in the upper stratigraphic column. Thus, 100 ms of two-way time was translated to 100 m of sediment. Raw isopach data were recorded in milliseconds; maps and discussion are presented in meters.

Piston and kasten cores were collected to verify seismic facies (Fig. 2), define the LGM position (Domack et al., 1999a; Licht, 1995; Licht et al., 1995, 1996, 1999), construct stratigraphic models of environmental changes subsequent to deglaciation (Domack et al., 1995a, 1995b, 1999a; Cunningham et al., 1999; Jennings et al., 1995), and provide a radiocarbon chronology of deglaciation and environmental changes (Domack et al., 1995a, 1995b, 1999a; Licht, 1995; Licht et al., 1996; Cunningham et al., 1999; Franceschini, 1995; Hilfinger et al., 1995). Domack et al.'s companion paper in this issue (1999a) presents results of a detailed sedimentological, geochemical, and stratigraphic investigation of the Ross Sea cores collected during the 1994 and 1995 cruises.

RESULTS

Regional Geomorphic Setting

As stated previously, a series of northeast-southwest–trending highs and lows characterizes the Ross Sea floor. Seismic profiles collected parallel to the shelf break (i.e., approximately northwest-southeast strike profiles) across the Mawson-Crary and Pennell-Iselin-Ross bank complexes in the western Ross Sea reveal that the banks are steep sided, with stepped flanks and essentially flat tops that dip gently to the east (Figs. 2 and 3). A rim or ramp often occurs at the bank edges. The banks range from 40 to 130 km in width and rise to within 250 m of the sea surface. Measured bank-crest to trough-base reliefs range from 170 to 200 m. Internal bank stratification is horizontal to gently inclined, with reflectors commonly being truncated by erosion in the troughs (Fig. 3). Strata forming the banks are predominantly Miocene in age (Anderson and Bartek, 1992). A layer of thin to isolated patches of modern sediment overlies the bank tops (Domack et al., 1999b). This material displays a hummocky external character and a chaotic internal signature. On strike seismic sections across the banks of the middle to outer shelf of the western Ross Sea, wedges of acoustically massive recent material, with occasional clinoforms, extend from the bank edge and downlap into the trough (Fig. 4).

Two distinct troughs occur in the western Ross Sea, marked by the Victoria Land–Drygalski basins and the JOIDES–Central Basins (Fig. 2). The troughs are foredeepened; inland depths exceed 900 m, and the shelf break occurs at approximately 500 m. The troughs are ~45–65 km wide and reach depths of 600 m on the middle shelf. They join landward, broadening and deepening. Seismic records across the inner shelf record seaward-dipping strata truncated at the sea floor. Deep Sea Drilling Project (DSDP) drill site 273, located in the northern Central Basin, sampled lithified Miocene and older glacial sediment (Fig. 2; Hayes and Frakes, 1975). Seismic stratigraphic investigations revealed a seaward-thickening wedge of Pliocene–Pleistocene strata resting above Miocene strata on the outer shelf, north of site 273 (Anderson and Bartek, 1992). These strata underlie the deposits investigated in this paper. Locally, thin patches of younger deposits occur above the Miocene strata on the inner shelf; these deposits are thicker in the troughs on the middle and outer shelf.

In contrast to the wide, flat-topped banks of the western Ross Sea, strike sections across the central and eastern Ross Sea record ridges trending northeast-southwest (Fig. 2). The term ridge is used, rather than bank, because of differences in depth and internal and external geometry; ridges are rounded and tend to occur in deeper water (Fig. 5). Ridge widths range from 35 to 60 km, with ridge-crest to trough-base relief measuring 60–135 m. The Central High ridge displays westward-prograding clinoforms within an overall chaotic seismic signature (Fig. 5). It is bounded by erosional unconformities and capped by a thin hummocky sediment layer. Two other ridges, with eastward-dipping clinoforms, an overall massive to chaotic internal geometry, and erosional bounding surfaces, have been observed in the eastern Ross Sea on lower-resolution seismic data (Alonso et al., 1992; Anderson et al., 1992; Shipp and Anderson, 1994a; Shipp and Anderson, 1995).

Troughs in the central and eastern Ross Sea also are foredeepened but are shallower (600–700 m deep) and broader (150–240 km wide) than the troughs of the western Ross Sea. The troughs are underlain by thick, seaward-prograding strata, interpreted by Alonso et al. (1992) to be Pliocene–Pleistocene glacial and glacial-marine deposits separated by glacial-erosional unconformities. DSDP Leg 28 drill sites 270, 271, and 272, from the flank of Central High, cored predominantly unlithified Pliocene–Pleistocene strata in the upper part of the stratigraphic section (Hayes and Frakes, 1975). The surface unit within the troughs, of interest in this study, forms sheets of material that thicken seaward.

Small-Scale Surface Morphology

The distribution of surface features observed in the multibeam and side-scan sonar data are summarized in Figure 6. Two primary patterns emerge; streamlined features occur in the troughs, and arcuate features occur on the bank tops and outer shelf. Streamlined features can be subdivided into lineations and teardrop-shaped highs.

Lineations. Multibeam images reveal that lineations, aligned roughly parallel to trough axes, cover much of the surveyed sea floor (Figs. 6 and 7). These features trend from N0°E to N56°E, with an average of N28°E (Fig. 7). Individual lineations extend in excess of 20 km and exhibit crest-to-crest spacing ranging from 300 to 650 m. In the western Ross Sea lineations are observed to within 85 km of the shelf edge. In the central Ross Sea lineations occur across the sea floor to within 45 km of the shelf break (Fig. 6). At depths <550 m (rarely at 600 m) in the western and central Ross Sea, the lineations are cross-cut or replaced by random, arcuate to straight grooves of varying width and depth. It is possible that the lineations extended farther north, but have been obliterated by the grooves.

The lineations in the Ross Sea are interpreted to be flutes and furrows of subglacial origin. A similar linear fabric is reported from other glaciated environments, although typically the features are smaller in scale (e.g., Barnes, 1987; Solheim et al., 1990; Josenhans and Zevenhuizen, 1990). C. D. Clark (1993, 1994) subdivided large-scale flutes associated with the Laurentide ice sheet into (1) megaflutes with lengths of 0.2–2 km and spacing of 20–400 m; and (2) mega-scale glacial lineations with lengths typically from 8 to 70 km, widths of 200–1300 m, and spacing of 0.3–5 km. The Ross Sea lineations fall within the range of length and spacing of C. D. Clark's (1993, 1994) subglacial mega-scale glacial lineations. This paper refers to the Ross Sea features as "mega-scale glacial lineations."

Drumlins. A region of teardrop-shaped bathymetric highs occurs on the inner shelf of the central Ross Sea in the Eastern basin trough (Figs. 6 and 8). The features trend N38° to 40°E, and taper in a seaward direction. Individual features range from 0.5 to 0.75 km in width and 3 to 8 km in length. Heights range between 40 and 100 m. Some exhibit a well-developed moat rimming the hill. The features are characterized by a strong surface return with a hummocky external geometry of long wavelength and high amplitude; internal stratigraphy is poorly imaged on seismic records. The acoustic basement can be traced along seismic profiles to DSDP site 270, where the basement consists of dolerite (Fig. 2; Hayes and Frakes, 1975; Anderson and Bartek, 1992). The features appear to be rock cored with a thin to absent cap of sediment. The highs are part of a geomorphic progression, landward to seaward, from relatively smooth bathymetry to mega-scale glacial lineations (Fig. 8). These features are interpreted to be drumlins or rock drumlins in the terminology of Sugden and John (1976), although the Ross Sea features are narrower and higher. They are similar in scale and form to drumlins identified by other investigators (e.g., Attig et al., 1989; Lundqvist, 1989; Boyce and Eyles, 1991).

Arcuate Grooves. Overprinting the mega-scale glacial lineations on the outer shelf are arcuate grooves (Figs. 6 and 9). These features commonly occur in water depths less than 550 m and rarely in water depths between 600 and 550 m. They are prominent on the banks and ridges, and on trough flanks (Fig. 6). The largest grooves are 1200 m wide and 30 m deep. More typically measured widths and depths fall in the ranges of 10–200 m and 5–15 m, respectively. The majority of these features are less than 10 km long. Side-scan sonar data recorded complex patterns of crisscrossing arcs that terminate abruptly (Fig. 9A). Chirp-sonar and subbottom-profiler records show depressions bounded on either side by steep-sided mounds of varying height (Fig. 9B). Often the deeper depressions and mounds are draped by a thin transparent unit (Fig. 9B). Shallower features are less frequently draped.

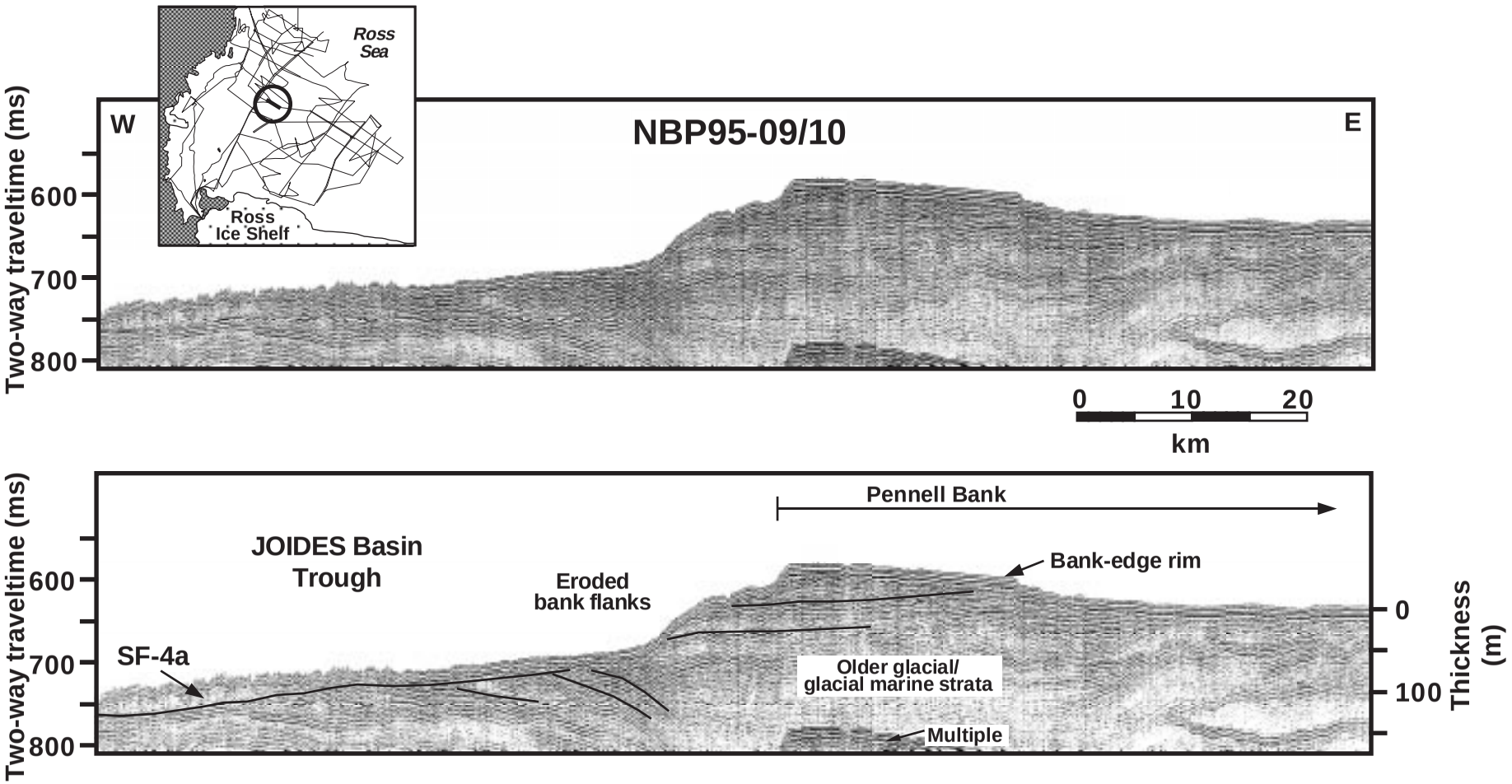

Figure 3. Strike-oriented profile using 50 in^3 (819.5 cm^3) airgun across trough flank and onto the Pennell Bank in the western Ross Sea. Note the truncated reflectors of older strata close to the surface. The bank top exhibits a tilt to the east. A bank-edge rim occurs at the bank margin. A thin layer of sedimentary material, interpreted to be Last Glacial Maximum deposits, occurs on the bank flank and within the trough. Location indicated on inset map. Acquisition and processing parameters are outlined in Table 1.

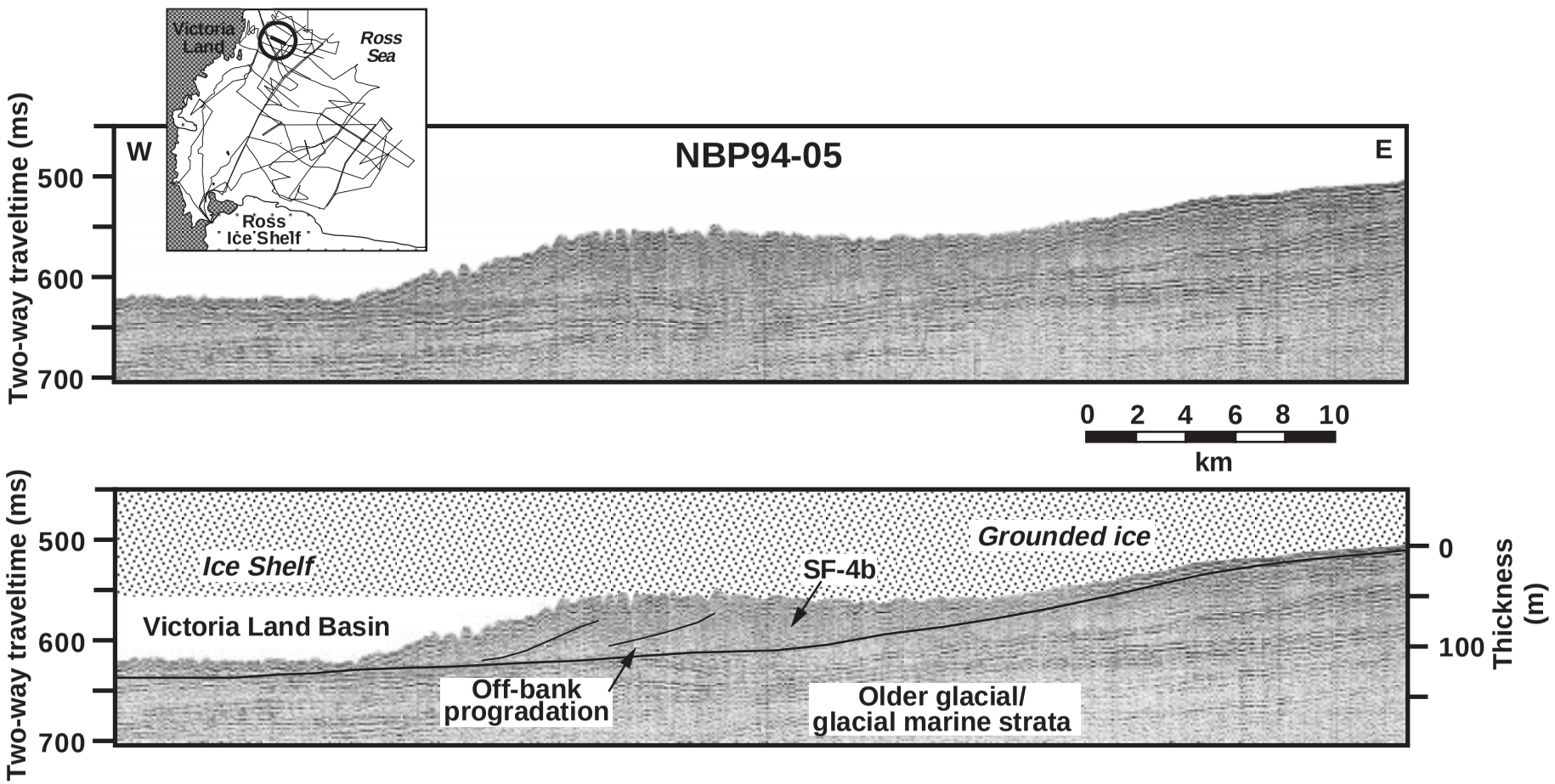

Figure 4. Strike-oriented profile using 50 in^3 (819.5 cm^3) airgun across a sediment wedge extending from Mawson Bank and downlapping into the Victoria Land Basin. Clinoforms within the wedge indicate lateral accretion from the east. Hypothetical grounded ice and ice shelf suggest the depositional setting of the sediment wedge. The section was chosen as a good representative of a geomorphic feature; the strata occur north of the Last Glacial Maximum deposits interpreted in this paper. Location marked on inset map. Acquisition and processing parameters are outlined in Table 1.

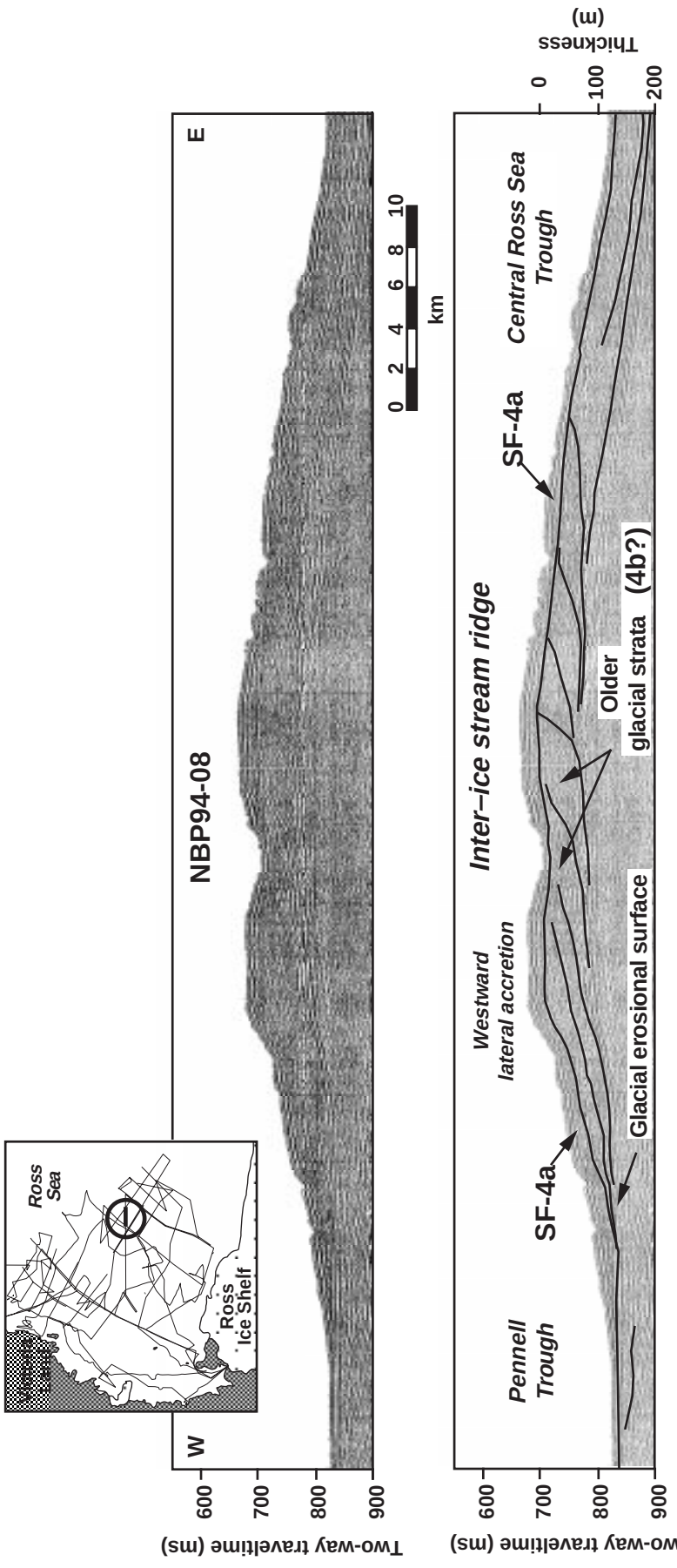

Figure 5. Strike-oriented seismic transect using 50 in^3 (819.5 cm^3) airgun across a trough-bank-trough system in the central Ross Sea. In contrast to the erosional flanks of the western Ross Sea banks, inter–ice-stream ridges of the central and eastern Ross Sea are depositional. Lateral accretion observed in the ridges is interpreted to indicate lateral shifting of extended paleo-ice streams as they flowed along the troughs. Location indicated on inset map. Acquisition and processing parameters are outlined in Table 1.

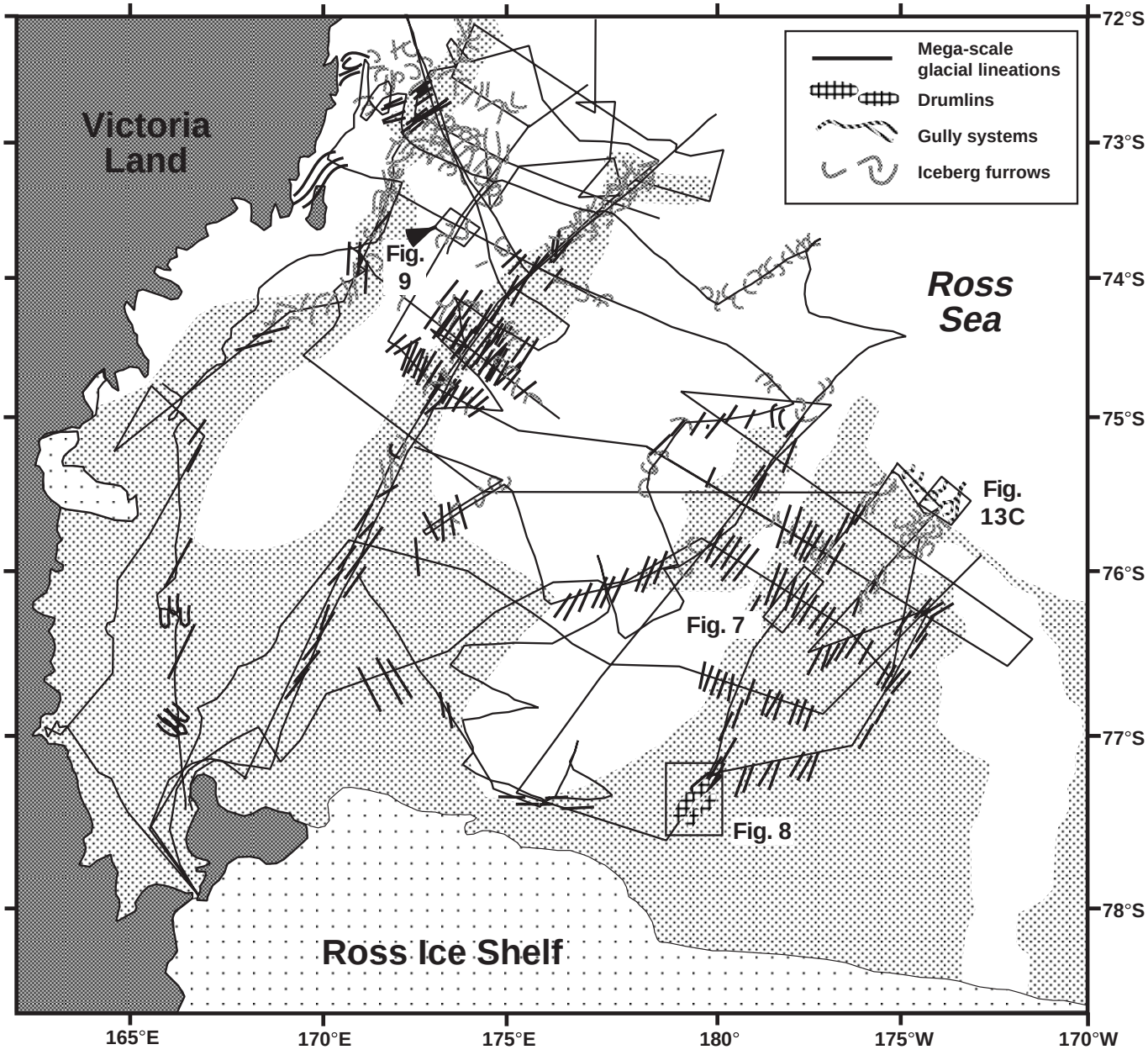

Figure 6. Schematic of features observed on swath bathymetry data. The features are located and oriented correctly; the size is exaggerated. Boxes depict locations of swath bathymetry data illustrated in this study.

The grooves are interpreted to be iceberg furrows, carved by iceberg keels impacting and plowing the sea floor. Similar features are observed off the Wilkes Land margin by Barnes (1987), on the Antarctic Peninsula shelf (Pudsey et al., 1994), and on other glaciated shelves (e.g., Josenhans and Zevenhuizen, 1990; Solheim et al., 1990; Syvitski et al., 1996), although the Ross Sea features appear to be larger than those described elsewhere. Modern icebergs with drafts of 330 m have been observed in the Ross Sea (Orheim, 1980); theoretical calculations place drafts of modern Ross Sea icebergs to almost 500 m (Barnes and Lien, 1988; Lewis and Bennett, 1984).

Seismic-Stratigraphic Units

Five seismic facies and their relative associations define the uppermost stratigraphy of the Ross Sea region (Fig. 10). The characteristics and interpretations of the facies, organized by relative age from youngest to oldest, are summarized in Table 2. The interpreted stratigraphic relationships are summarized as a diagram (Fig. 10G).

Seismic Facies 1. A 2–9-m-thick, widespread, transparent unit drapes all other seismic facies (Fig 10A). The upper surface is the sediment-water interface. On side-scan sonar records, arcuate iceberg furrows cut into the

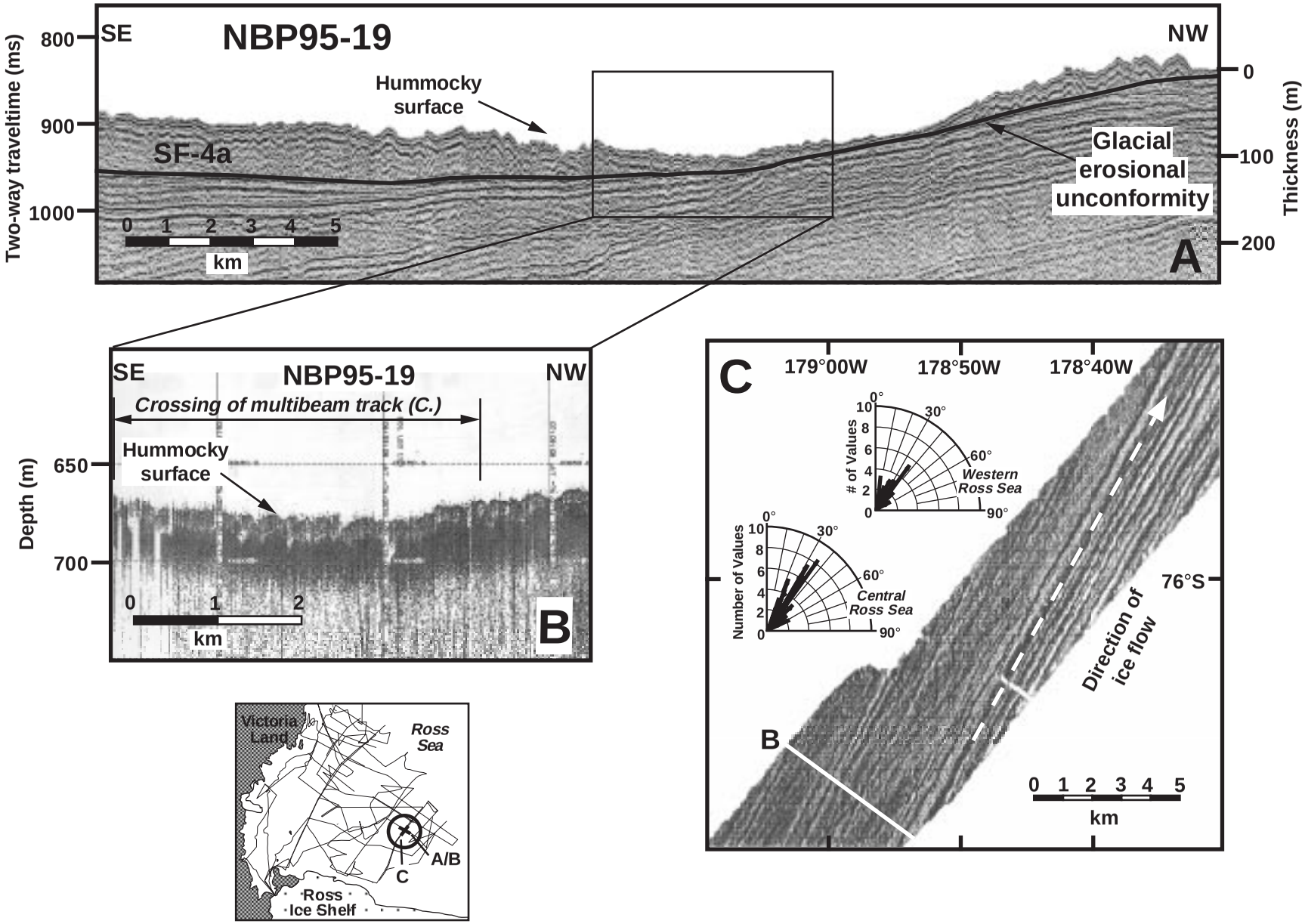

Figure 7. (A) Seismic transect using 50 in^3 (819.5 cm^3) airgun crossing mega-scale glacial lineations. The lower bounding surface is a glacial erosional unconformity. The hummocky nature of the upper surface is characteristic of fluted regions. Location of the profile is indicated in the inset map. Boxed region shows location of the 3.5 kHz crossing. (B) A 3.5 kHz transect illustrating details of hummocky upper surface. Region of the swath bathymetry crossing is shown. (C) Multibeam record crossing features interpreted to be mega-scale glacial lineations. The rose diagrams show measured directions of lineations and number of observations from swath bathymetry of the Ross Sea floor, divided into the western and central Ross Sea regions. Position of the 3.5 kHz crossing is indicated with a solid white line. Figure 6 shows the location of the swath bathymetry data and also distribution of similar lineations within the constraints of the data set. Acquisition and processing parameters for all data sets are outlined in Table 1.

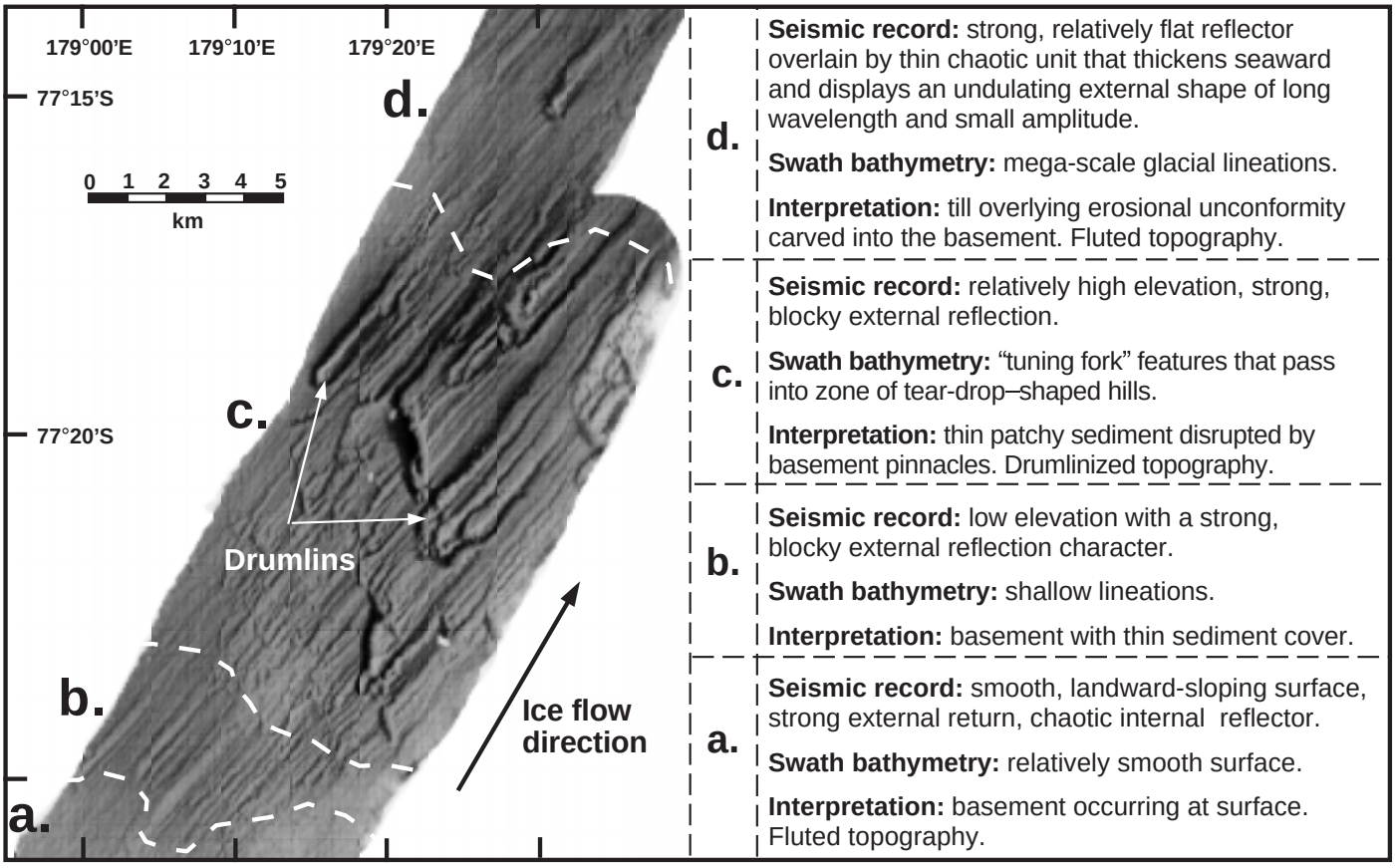

Figure 8. Multibeam record of drumlins on the inner shelf of the central Ross Sea. The drumlins merge into mega-scale glacial lineations to the north. Text describes the observed transition of geomorphic features and interpretation. Figure 6 displays the location of the drumlins and the image. Acquisition and processing parameters are outlined in Table 1.

unit, occasionally removing it from the stratigraphic section. Seismic facies 1 is observed to infill iceberg furrows as well (Fig. 10A). The unit occurs in troughs on the basis of CHIRP sonar data, selected subbottom profile records, and cores. A complete picture of the distribution is difficult because of the thinness of the unit and the lower quality of earlier subbottom records. Piston and kasten cores that penetrated this unit recovered diatomaceous mud and/or ooze (Domack et al., 1999a). Seismic facies 1 is interpreted to be an open-marine deposit.

Seismic Facies 2. A thin (<15 m), geographically restricted sheet of acoustically subdued massive material occurs on the middle shelf (Fig. 10B). The lower bounding surface is relatively smooth and flat. The upper surface is smooth to hummocky. Hummocks often are organized into consistent, low-amplitude, high-frequency bedforms that display parallel, straight-crested signatures on side-scan sonar data (Fig. 10B). Swath bathymetry data recorded mega-scale and smaller glacial lineations across the surface of the unit. This unit occurs only in association with seismic facies 3 within JOIDES Basin (Fig. 11); its outer limit downlaps onto seismic facies 3. Cores penetrated a soft diamicton with foraminifers, the equivalent of lithofacies D2 of Licht et al. (1999). Seismic facies 2 is interpreted to be an ice-proximal glacial-marine unit that has been overridden by the ice sheet (Domack et al., 1999a). It may represent a deformational layer (folds?) formed under the ice sheet at the ice-substrate interface.

Seismic Facies 3. Seismic facies 3 is a geographically restricted sheet of massive material <35 m thick. It has a subdued signature and rests on seismic facies 4a or 5 (Figs. 10C and 11). The upper surface is smooth to hummocky in cross section. Mega-scale glacial lineations characterize the surface. Seismic facies 3 occurs only on the middle shelf within the trough of JOIDES Basin (Fig. 11). Piston cores penetrated a soft diamicton with foraminifers. Seismic facies 3 is interpreted to be an ice-proximal glacial-marine unit that has been overridden by the ice sheet (Domack et al., 1999a).

Seismic Facies 4a and 4b. Seismic facies 4 is observed on all scales of data and is the most widespread unit in the study region. It is characterized internally by a massive to chaotic acoustic signature with rare clinoforms. This facies is bounded on the lower surface by a strong, regional, erosional unconformity. The upper surface commonly displays a disorganized hummocky character with frequent hyperbolic returns (Fig. 10D). Individual hummocks range between 5 and 15 m in amplitude (crest to trough). Seismic facies 4 is divided into two subfacies, 4a and 4b. They are identical in acoustic character, but stratigraphically distinct. Seismic facies 4b, bound by erosional unconformities, underlies all other seismic facies, including seismic facies 4a (Fig. 10E).

Seismic Facies 4a. Seismic facies 4a is draped by seismic facies 1 and downlaps seismic facies 5. The lateral relationship with seismic facies 2 and 3 is less clear, although seismic facies 4a downlaps onto facies 2 and 3 in some settings; deposition is believed to be time transgressive. Distribution of seismic facies 4a is patchy; primary concentrations occur within the troughs on the middle to outer shelf (Fig. 11). Thin, patchy accumulations <10 m across occur on the inner shelf and on bank tops. Piston cores within

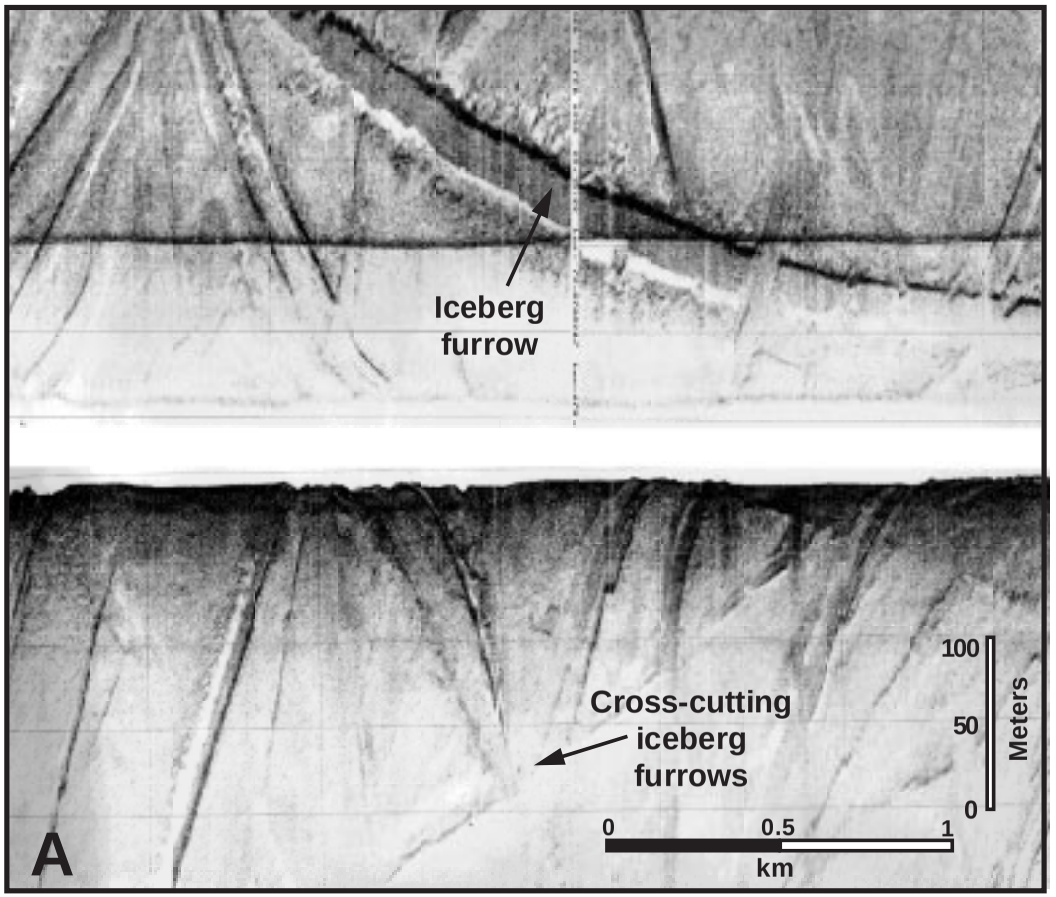

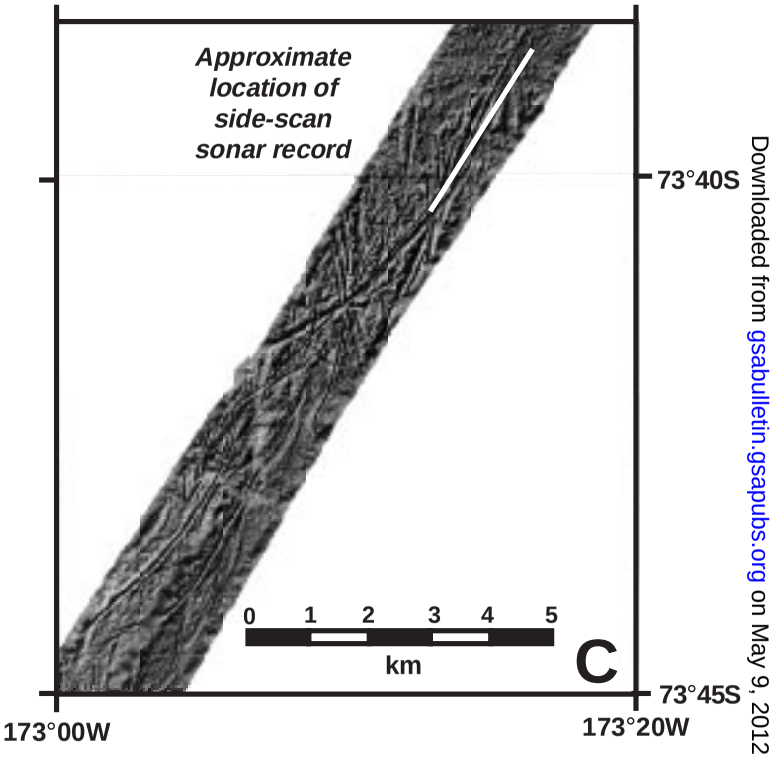

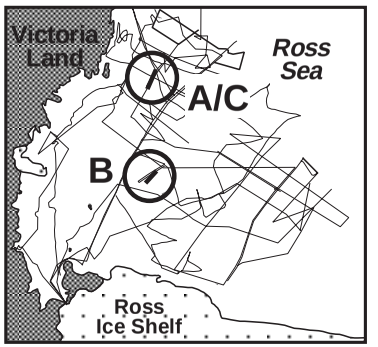

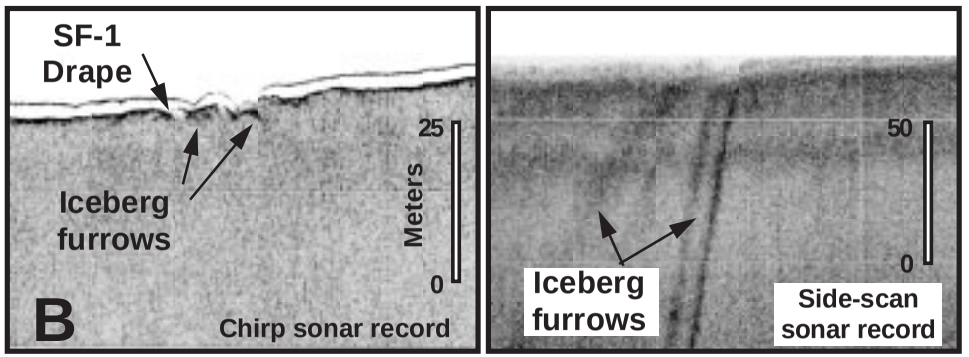

Figure 9. (A) Side-scan sonar record of arcuate furrows on the outer shelf of the central Ross Sea. The lightness of a portion of the upper channel is an artifact of data collection. (B) CHIRP-sonar and associated side-scan sonar record of sediment-draped furrows occurring in the troughs. (C) Swath bathymetry crossing of Mawson Bank in the vicinity of Figure 9A. Note the multiple scales, arcuate patterns, and cross-cutting relationships of the furrows. The furrows are interpreted to result from the drafts of icebergs impacting and moving along the sea floor. Table 1 outlines acquisition and processing parameters. Figure 6 displays the distribution of similar features within the constraints of the data set and the location of C.

this seismic facies penetrated a stiff, pebbly, sandy mud (diamicton), interpreted to be subglacial in origin, based on criteria outlined by Domack et al. (1999a) and in Anderson (in press). Based on seismic character and geometry, surface features, and correlation with core material, the acoustically massive units are interpreted to be subglacial till (Fig. 10D; e.g., King and Fader, 1986; McCann and Kostaschuk, 1987; Solheim et al., 1990; Belknap and Shipp, 1991; King et al., 1991; Licht et al., 1999; Domack et al., 1999a). Seismic facies 4a exhibits a variety of external geometries, including small mounds, intratrough wedges, intratrough sheets, attached-flank wedges and lenses, and back-stepping ridges, described later.

Seismic Facies 4b. Facies 4b underlies seismic facies 5 and directly underlies facies 4a (Fig. 10, D and E). It crops out at the sea floor seaward of facies 5. Its surface character is hummocky at the sea floor and beneath laminated facies 5. Mega-scale glacial lineations occur in these regions. However, where the unit is interpreted to occur beneath seismic facies 4a, the upper and lower bounding surfaces are smooth and flat. Seismic facies 4b occurs on the outer shelf of western and central Ross Sea. Landward, the facies is truncated by a glacial-erosional unconformity. Piston cores sampled very compact diamicton with rare, probably reworked, foraminifers. Like facies 4a, seismic facies 4b is interpreted to be subglacial till.

Subunits of Seismic Facies 4a Based on Geomorphology and Location. *Mounds.* Seismic facies 4a occurs as small mounds and thin wedges (<5 m) across the banks and inner shelf of the Ross Sea (Fig. 12, A-I and B). The accumulations are discontinuous. They display a hummocky surface that correlates with mega-scale and smaller glacial lineations and, in the shallower regions, iceberg furrows.

Intratrough Wedges. In JOIDES Basin seismic facies 4a assumes a wedge-like geometry within the center of the trough (Fig. 2; Shipp and Anderson, 1995; Shipp et al., 1995). The distinct wedge overlies an erosional unconformity (Fig. 12A). It extends 40 km along the trough axis, reaches a maximum thickness of 80 m, and thins in landward and seaward directions. Intermediate-resolution seismic data display rare, stacked concave-down reflectors within the predominantly acoustically massive interior. The internal reflectors dip seaward with an approximate apparent angle of 0.2°. The crest and landward flank of the wedge display a hummocky surficial character (Fig. 12, A-II and C).

Karl et al. (1987) mapped a 0–40-m-thick unit, interpreted to be basal till, in the western Ross Sea. The package rested on a regional paraconformity to angular unconformity interpreted to have been eroded by an expanded ice sheet. Although the study region did not extend as far north or east as this study, the distribution of the seismic unit described by Karl et al. (1987) appears to correlate with seismic facies 4a in the western Ross Sea in this investigation. The difference in thickness observed in the two studies may result from the location of seismic profiles.

Intratrough Sheets. In contrast to the isolated wedges of the western Ross Sea, seismic facies 4a in the central Ross Sea trough occurs as two sheets separated by a zone of nondeposition. The landward sheet extends 80 km from the middle shelf toward the outer shelf and thickens in a seaward direction from <10 to ~50 m, eventually pinching out (Fig. 11). A second sheet begins 50 km north of the pinch-out and extends to the continental-shelf edge. It also thickens in a seaward direction, from <10 to 60 m at the shelf break (Figs. 11 and 13A; Shipp and Anderson, 1994a, 1994b). Where the unit is present, a nearly flat erosional unconformity forms the lower surface; the upper surface is the sea floor and is characterized by hummocky topography. The hummocky surface correlates with mega-scale glacial lineations on the swath bathymetric data (Figs. 6, 9C, and 13A). At water depths shallower than 550 m, the lineations are absent or occur in association with arcuate grooves. A series of landward-dipping faults cuts and offsets the strata on some of the outer shelf dip lines, creating fault ramp folds at the surface (Fig. 13B). The angle of the planes steepens toward the outer shelf from approximately 1° to 2°. Small gullies, identified on swath bathymetry data, occur at the seaward extent of the wedge on the continental-shelf edge in the central Ross Sea (Fig. 13C). These features begin abruptly and develop into deep channel systems in less than a kilometer. Observed gullies extend ~6.5 km. At their maximum the gullies reach widths of 700 m and depths of 45 m. The gullies coalesce downslope into wider channels and are observed to diverge and extend into small fans where the gradient decreases.

Attached Flank Wedges and Lenses. Seismic facies 4a also comprises wedges that are attached to the bank flanks and downlap into the trough (Fig. 4). In some settings the wedges are flat topped, essentially extending the bank. In other locations the material assumes a lens shape on the bank flank. Clinoforms indicate lateral accretion from the bank into the trough. The wedges are <60 m thick and extend <30 km from the bank to the trough. The wedges downlap onto seismic facies 3, 4a, 4b, or 5.

Back-Stepping Ridges. A series of parallel, 25–50-m-high ridges were observed on seismic profiles and swath bathymetry data across an 85-km-wide region of the eastern and southern margin of the northern Pennell Bank (Figs. 14 and 15). The ridges are interpreted to "ring" the Pennell Trough, although the swath bathymetry data do not cover the entire region. The ridges are asymmetric, with the steep side facing the trough and the more gentle gradient sloping toward the bank (Fig. 15). The ridges are younger to the west, toward the bank, based on downlap patterns observed in the toes of the features (Fig. 15). Faint lineations, or flutes, perpendicular to the ridge trend, occur between the ridges. The ridges downlap seismic facies 5 or a glacial-erosional surface (Fig. 14C).

Seismic Facies 5. Seismic facies 5 is comprised of thin, acoustically laminated, ponded and draping deposits (Fig. 10E). The facies reaches approximately 10 m in thickness with individual "laminations" of 1–2 m. The ponded deposits, observed rarely, occur at the base of the facies and partially infill the underlying hummocks. Seismic facies 5 immediately underlies seismic facies 3 and 4a. It drapes seismic facies 4b, mimicking the hummocky surface character, and ultimately pinches out against facies 4b on the outer shelf (Fig. 10F). Seismic facies 5 occurs at the surface (overlain by seismic facies 1) in two basins, JOIDES and Pennell Trough, and tentatively is identified in Victoria Land Basin (Fig. 11). The exact landward extent of seismic facies 5 is obscured by overlying deposits. Lower-resolution airgun data help clarify a maximum landward position. Cores acquired from seismic facies 5 contain a complex stratigraphy of interbedded diatomaceous mud and/or ooze, silty clay, granulated facies, foraminifer-rich sand, and soft diamicton (Domack et al., 1999a). The seismic unit is interpreted to be glacial marine, with possible sub–ice-shelf facies and open-marine units.

INTERPRETATION

Facies Associations

The seismic facies described earlier are interpreted to be organized into subglacial, grounding-line proximal, proximal and distal glacial-marine, and open-marine deposits associated with glacial expansion and subsequent retreat across the Ross Sea continental shelf. The western Ross Sea, Pennell, and central Ross Sea troughs hold the thickest and most complex accumulations of sediment. Deposits on the banks are less extensive (to absent). The distribution of facies and features in the troughs and across the banks leads to a reconstruction of the expanded ice system in the Ross Sea.

Western Ross Sea Troughs. The largest geophysical database exists for the JOIDES Basin–Central Basin trough (Fig. 2). All seismic facies are present and display complex stratigraphic relationships (Fig. 12). Patchy, thin wedges to mounds of seismic facies 4a exist on the inner shelf (Fig. 12, A-I and B). These deposits rest on a smooth erosional unconformity that separates them from the older seaward-dipping strata. The surface of facies

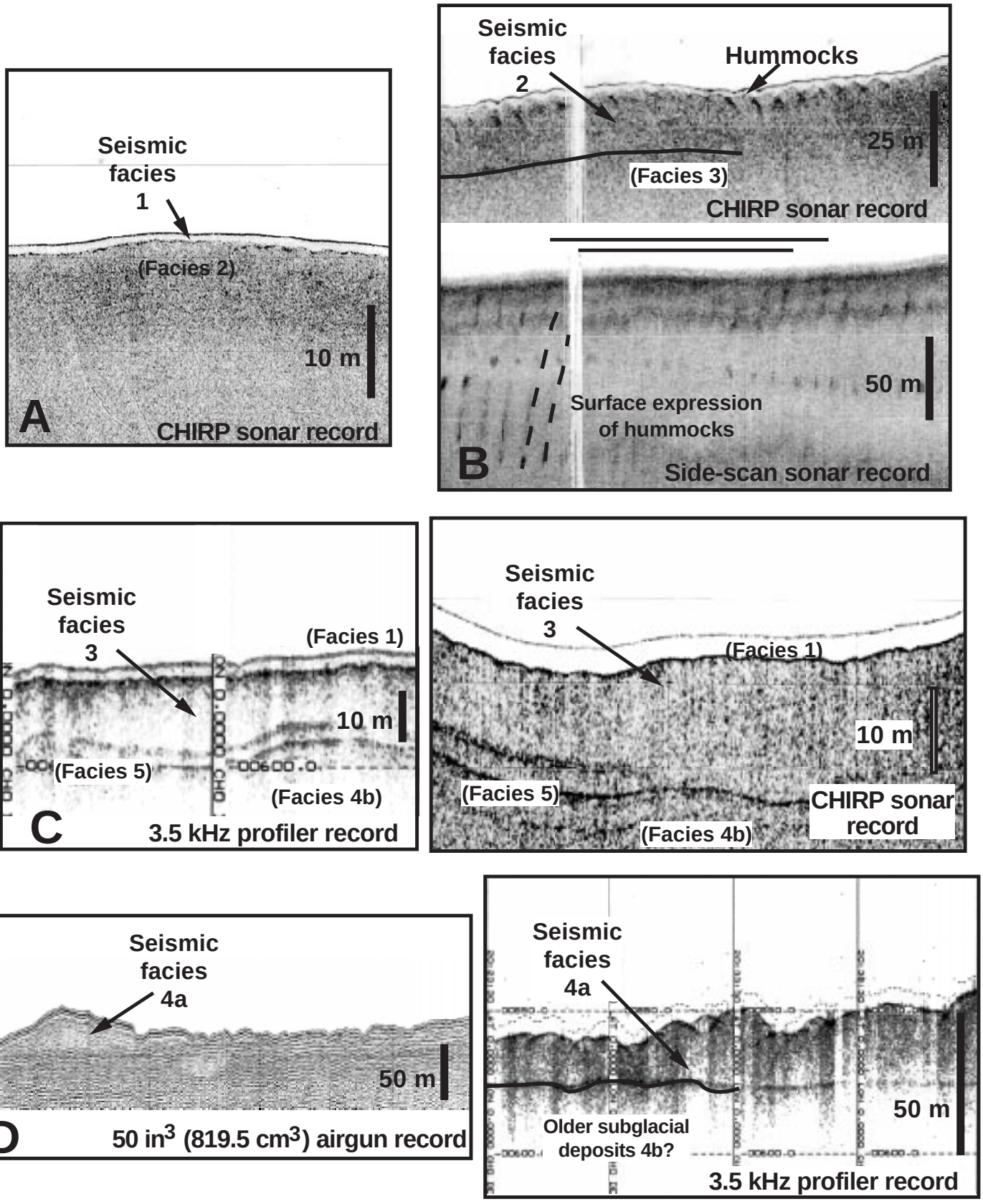

Figure 10. (A–F) Representative examples of seismic facies distinguished in this investigation. Data type is indicated on each panel. Table 1 outlines acquisition and processing parameters. Table 2 describes the seismic stratigraphic characteristics of the facies.

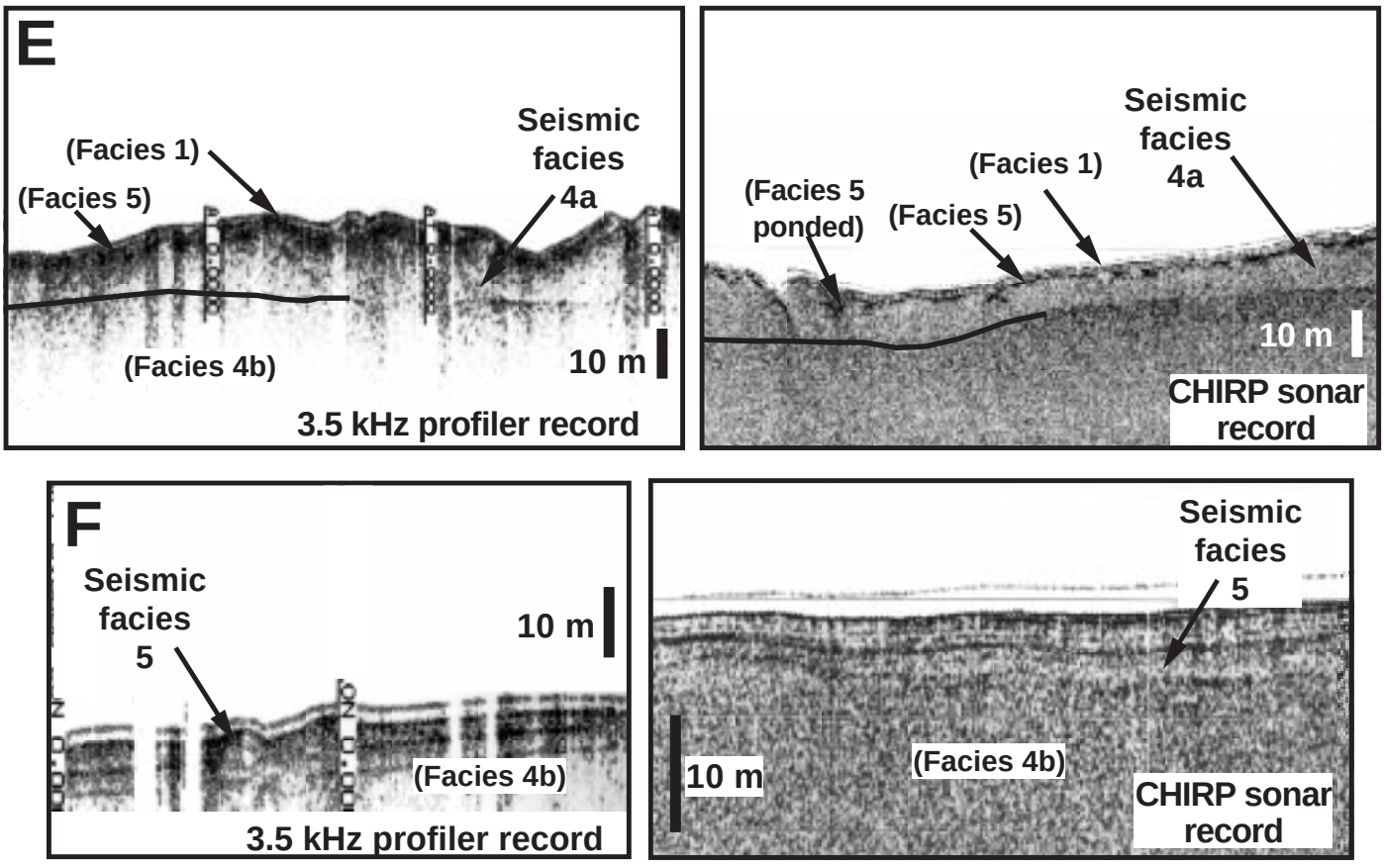

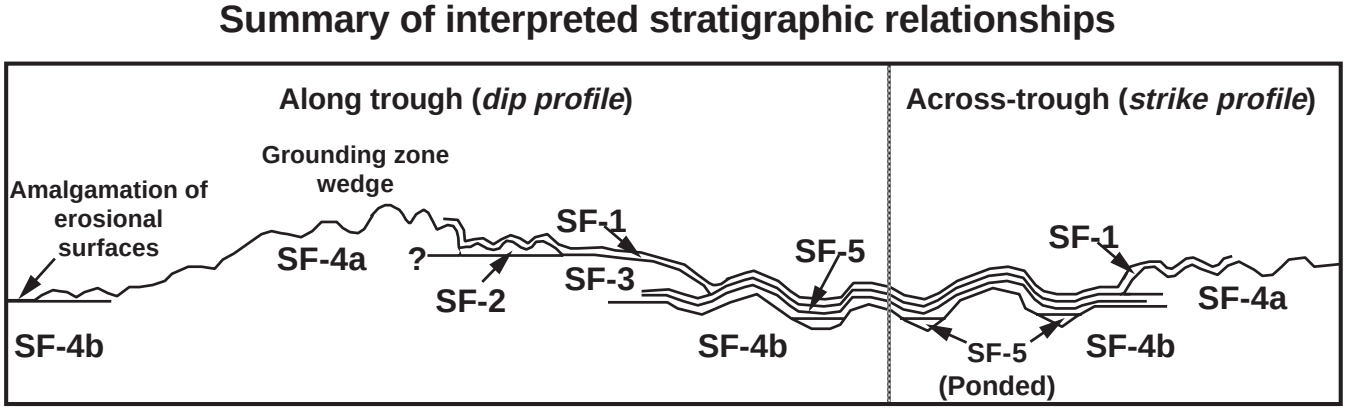

Figure 10. (*Continued*).

4a is heavily fluted and draped in many regions by a thin layer of facies 1. The deposits thicken to the larger intratrough wedge in the vicinity of Coulman Island (Fig. 12, A, A-II, A-III, C, and D). Seaward, seismic facies 4 is replaced by a sheet deposit comprised of seismic facies 2 stacked on seismic facies 3 (Fig. 12, A, A-IV, and E–H). The relationship between facies 4a and 3/2 is unclear; facies 4a downlaps facies 3 in many locations (Fig. 12A-III). Facies 2 pinches out against facies 3. Facies 3 extends as a wedge 70 km beyond the Coulman Island wedge and downlaps onto the draping, acoustically laminated deposits of seismic facies 5 (Fig. 12E). Sediment associated with facies 3 may become a layer within facies 5 deposits.

Swath bathymetry and CHIRP-sonar records show that mega-scale and smaller glacial lineations cut across the surfaces of facies 2, 3, and 4a (Fig. 12, A-II, C, and D). Arcuate iceberg furrows are prominent, concentrated on the wedge crest (Fig. 12A-II). Facies 5 drapes facies 4b and reflects the fluted nature of the lower facies 4b. Facies 5 remains close to the surface for 70 km, eventually pinching out against seismic facies 4b. Seismic facies 5 and 4b can be traced landward, under facies 2, 3, and 4a, for a short distance. Eventually they are truncated; the erosional surface beneath facies 5 and 4b converges with the truncated surface beneath facies 4a. Seismic facies 4b is interpreted to extend seaward toward the shelf break. The surface is fluted and increasingly iceberg furrowed in the shallower seaward regions (Fig. 12H). Facies 1 overlies facies 5 and 4b on the middle shelf to outer shelf. These facies are absent on the outermost shelf, a fact attributed to intense iceberg scouring and/or resuspension or nondeposition resulting from currents.

TABLE 2. SEISMIC FACIES

Unit	Internal acoustic geometry	External geometry and bounding surfaces	Defining database	Interpretation (this study)	Correlation to Domack et al. (this issue)
1	Transparent	Draped fill	Subbottom profiler; CHIRP sonar; cores	Open marine; diatomaceous mud	Diatomaceous mud and/or ooze
2	Massive; subdued	Sheet;	Subbottom profiler; CHIRP sonar; cores Low-amplitude, high frequency hummocky upper surface; Smooth, erosional lower surface	Glacial marine in origin; Ice proximal; Overridden by ice sheet	Glacial marine diamicton (and other units) (Core resolution is higher than seismic resolution)
3	Massive; subdued	Sheet; Smooth to hummocky upper surface; Smooth, erosional lower surface	Subbottom profiler; CHIRP sonar; cores	Glacial marine in origin; ice proximal; Overridden by ice sheet	Glacial marine diamicton (and other units) (Core resolution is higher than seismic resolution)
4a	Massive to chaotic; Common hyperbolic reflectors; Rare clinoforms	Wedges, mounds, lenses; Hummocky upper surface w/ frequent hyperbolic returns; Smooth, erosional lower surface	Airgun; subbottom profiler; CHIRP sonar; cores	Subglacial diamicton	Subglacial diamicton
5	Laminated	Draped fill with ponded lower unit	Subbottom profiler; CHIRP sonar; cores	Open marine to sub–ice-shelf; May include older interglacial sediment	Interbedded open-marine and sub–ice-shelf facies
4b		Massive to chaotic; Common hyperbolic reflectors	Hummocky upper bounding surface; Flat, erosional lower` surface	Airgun; subbottom profiler; CHIRP sonar; cores	Subglacial diamicton N/A

Note: N/A = not available.

Radiocarbon stratigraphies in the region indicate that the deposits fall into two broad age groups. In general, north of Coulman Island, dates on carbonate components from outer shelf diamictons yield uncorrected ages older than ~20 k.y. B.P. (Reid, 1989; Domack et al., 1995a; Licht, 1995; Licht et al., 1995, 1996). South of this location, the dates are <20 k.y. B.P. Thus, on the basis of radiocarbon stratigraphies, the outer shelf diamictons were deposited prior to the LGM, and the middle and inner shelf lithofacies are related to the most recent glacial expansion (LGM) and subsequent retreat across the Ross Sea continental shelf.

Based on the seismic facies interpretation (Table 2; Figs. 10 and 12) and core data (Domack et al., 1999a), seismic facies 4b is interpreted to be associated with a previous glaciation (pre–oygen-isotope Stage 2) in which ice extended to the continental-shelf edge, depositing a shelf-edge moraine. Subsequent to ice retreat, the draping, laminated deposits associated with seismic facies 5 were deposited in a sub–ice-shelf to open-marine environment. Grounded ice is interpreted to have advanced to the vicinity of Coulman Island and paused during the LGM, depositing the Coulman Island grounding-zone wedge. Clinoforms in the wedge indicate seaward progradation. The subglacial material was deposited at the ice edge into the marine environment. Ice-proximal glacial-marine deposits were deposited in front of the wedge, forming seismic facies 3. An ice shelf may have existed, resulting in continued deposition of sub–ice-shelf deposits in seismic facies 5. Alternatively, no ice shelf was present and open-marine sedimentation continued at the sites of facies 5 deposition. Ice advanced beyond the grounding zone across facies 3. As it advanced, it reworked the upper part of facies 3, creating facies 2. The flat surface between 2 and 3 represents the base of deformation; the upper fluted surface of facies 2 is the ice-contact plane. Seaward of facies 2, facies 3 is fluted, though faintly (compare Fig. 12, G and H). Radiocarbon ages in the glacial-marine sediment of facies 2 provided an uncorrected age of approximately 14 k.y. B.P. (NBP95-KC-39; Domack et al., 1999a, 1995a, 1995b; Licht, 1995; Licht et al., 1995, 1996; Cunningham et al., 1999; Hilfinger et al., 1995). This permits placement of the LGM extent at the northern edge of these deposits. The ice sheet then retreated, paused a second time at the Coulman Island grounding-zone wedge, and deposited facies 4a material that downlaps on the surface of facies 2. As the ice sheet retreated, large icebergs were produced. These carved the larger, deeper furrows into the grounding-zone crest and surrounding high regions. Only one large grounding-zone wedge is observed in the JOIDES–Central Basin trough. Small wedges and patches of material (<5 m) occur landward of the wedge. Thus, the inner shelf is interpreted to be a zone of erosion with thin deposits of subglacial material being transported toward the ice edge. The inner shelf has been the site of erosion for many glaciations; the erosional surface is an amalgamation of many glacial-erosional events.

The grounding-zone wedge shows striking similarities to a single “till tongue” of King and Fader (1986). Till tongues are wedge-shaped accumulations of acoustically incoherent material that form through the accumulation of subglacial debris carried to the grounding line of a marine-based ice sheet with a floating terminus (King et al., 1991). They interfinger with ice-proximal glacial-marine deposits; stacked till tongues indicate oscillations of the grounding line. The grounding-zone wedge described in this investigation is similar to King et al.’s (1991) till tongues in geometry and scale of the wedge, regional extent, and amalgamation of erosional surfaces on the shelf near the zone of deposition. The Ross Sea wedge does not show evidence for large-scale slumping or sediment gravity-flow processes, indicating deposition of the wedge in close proximity to the grounding line. In contrast to the till tongues of King et al. (1991), the Ross Sea grounding-zone wedges do not interfinger with well-defined glacial-marine deposits. Rather, the deposits are dominated by the subglacial and grounding-zone proximal diamictons. Ross Sea is a polar setting characterized by a paucity of meltwater; little glacial-marine material is deposited in this setting. Higher resolution seismic data may better resolve the relationships between thin glacial-marine deposits and the wedge.

The lack of stacked wedges, organized as advance and retreat till tongues,

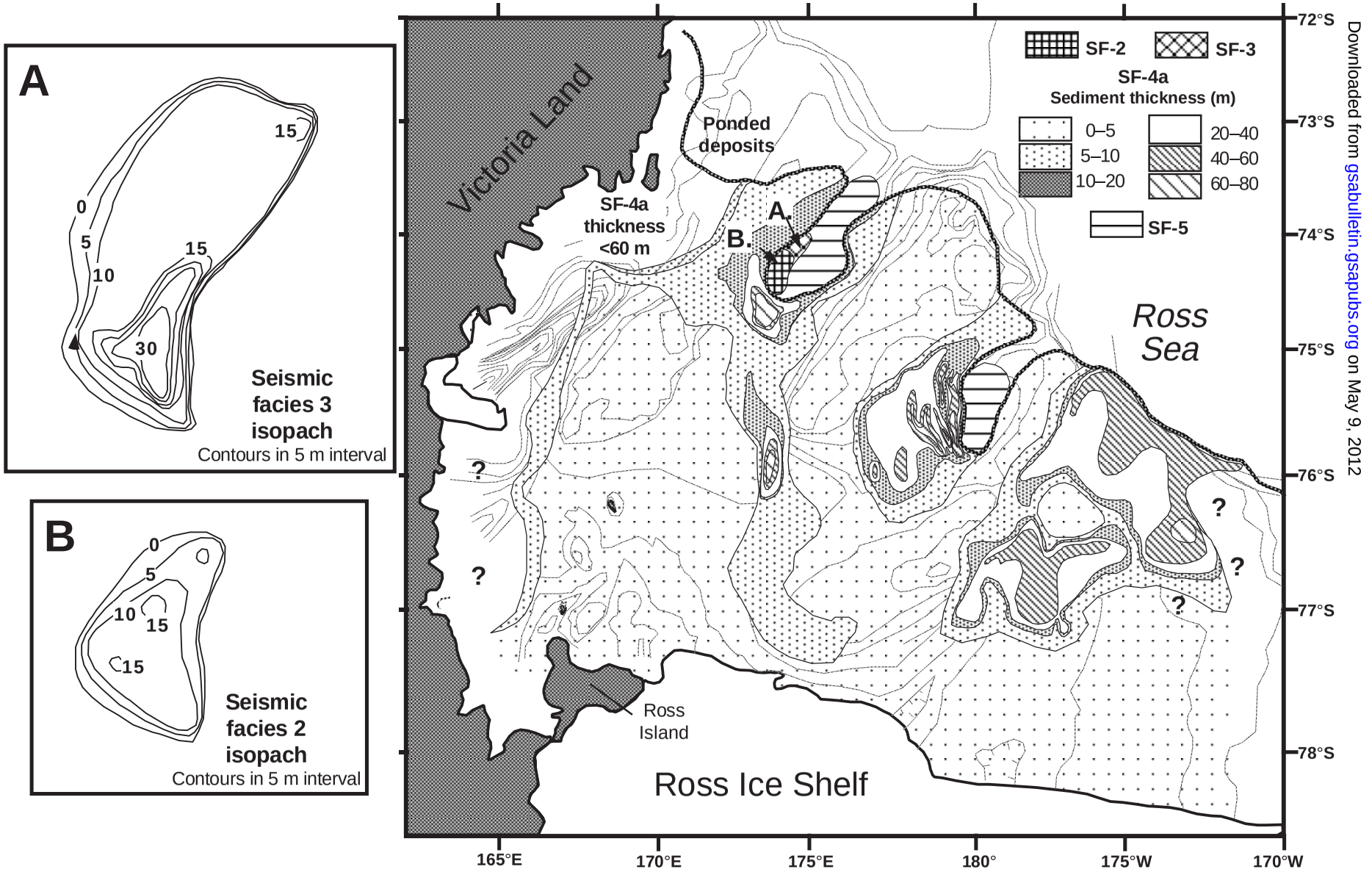

Figure 11. Distribution and isopach map of seismic facies 4a; contours variable to illustrate the presence of thin deposits. Note that significant deposits are restricted primarily to the outer troughs and around the bank edges. The Last Glacial Maximum grounding-line position is marked by a heavy line. Inset isopach maps of seismic facies 2 and 3 are in 5 m contour intervals. Facies are detailed in Figure 10 and Table 2.

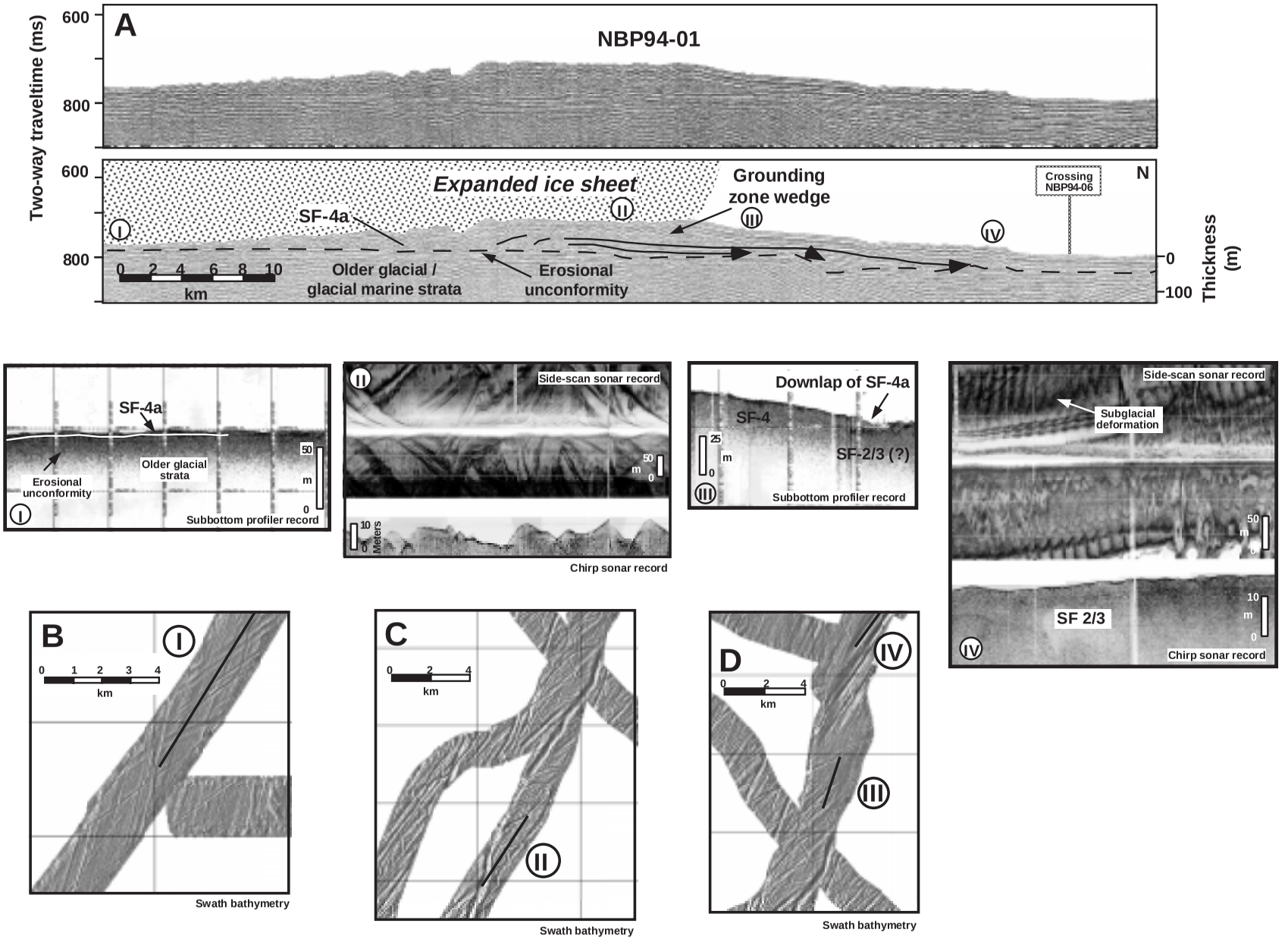

Figure 12. (A) Dip-oriented seismic profile using 50 in^3 (819.5 cm^3) airgun across the inner shelf grounding-zone position in the JOIDES Basin. On the basis of radiocarbon chronologies, the wedge marks the maximum position of the expanded ice sheet during the Last Glacial Maximum. Inset panels of CHIRP and 3.5 kHz data below the airgun profile correlate with encircled numbers posted on the seismic profile. These are higher-resolution data sets that illustrate seismic facies and relationships along the feature. (B, C, and D) Swath bathymetry data illustrating the regional sea-floor signature across the grounding-zone wedge. Corresponding positions of 3.5 kHz and CHIRP data insets are shown as heavy black lines annotated by encircled numbers.

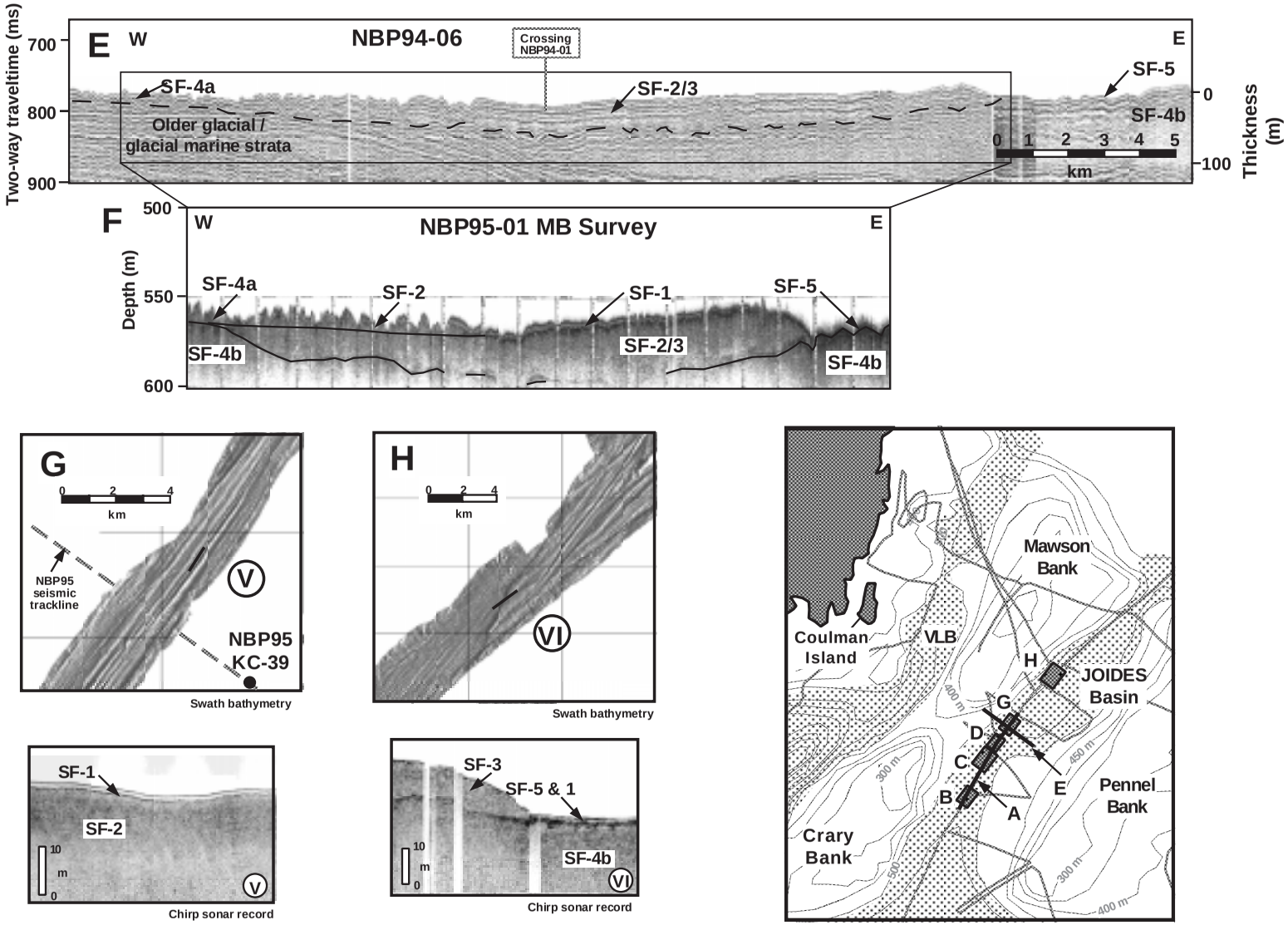

Figure 12. (*Continued*.) (E) Strike-oriented seismic profile using 50 in^3 (819.5 cm^3) airgun across the grounding zone in the ice-proximal region. Seismic track crossings are located on A and E. (F) The 3.5 kHz record, coincident with strike section E, across the seaward edge of the feature. The higher-resolution record shows the thin, acoustically transparent seismic unit (SF-1) overlying the hummocky surface of the subdued massive units (SF-2/3) and the downlapping of the unit onto the older glacial surface (SF-4b). This thin drape continues in a seaward direction. (G) Swath bathymetry displaying mega-scale glacial lineations across the surface of seismic facies 2, north of the grounding-zone wedge, in the vicinity of kasten core NBP95-39 (Domack et al., 1999a). Associated CHIRP sonar record (V) shows the relationship between seismic facies 2 and 3 in this region. Position of CHIRP-sonar data is shown on the swath bathymetry as a bold black line. (H) Swath bathymetry data and associated CHIRP- sonar data (inset VI) over region where seismic facies 3 downlaps onto acoustically laminated seismic facies 5. Locations of swath bathymetry and 50 in^3 airgun profiles indicated on inset map. Acquisition and processing parameters are indicated in Table 1. Seismic facies (SF) are detailed in Figure 10 and Table 2.

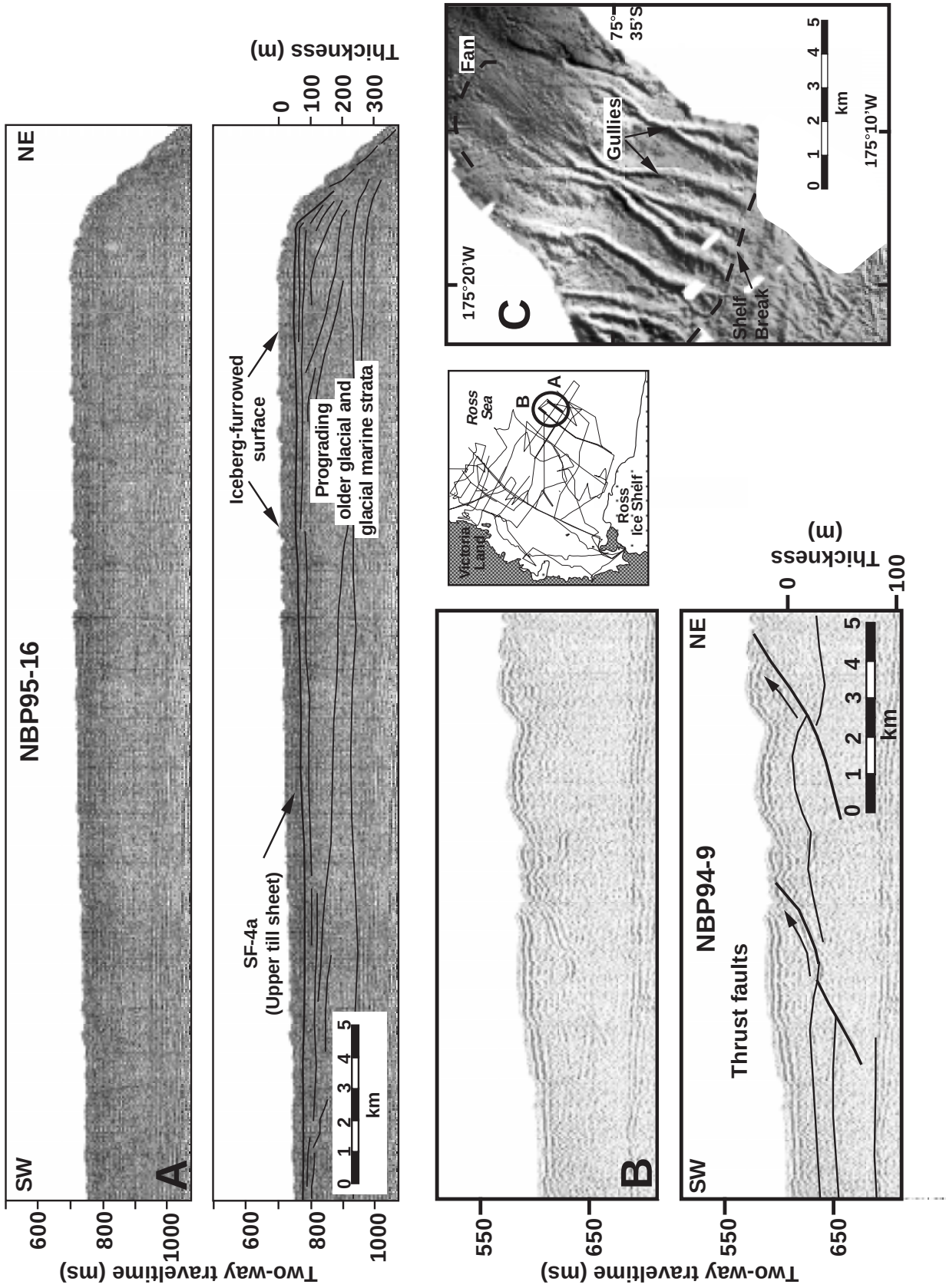

Figure 13. (A) Dip-oriented seismic profile using 50 in^3 (819.5 cm^3) airgun across the outer shelf of the central Ross Sea. Grounded ice is interpreted to have extended to the continental-shelf edge in this region. (B) Dip-oriented seismic profile using 50 in^3 airgun across the outer shelf of the central Ross Sea illustrating a series of thrust faults that offset the strata. The displacement of strata along the thrusts is interpreted to have resulted from increased pore-water pressures in impermeable beds (Bluemle and Clayton, 1984; Croot, 1987). (C) Swath bathymetry record of interpreted gullies at the shelf edge in the central Ross Sea. Figure 6 displays the distribution of similar features within the constraints of the data set and location of this image. Gullies are interpreted to indicate the presence of extended ice at the continental-shelf edge. A fan marks the location where the flow slowed. Locations indicated on inset map. Acquisition and processing parameters are indicated in Table 1. Seismic facies (SF) are detailed in Figure 10 and Table 2.

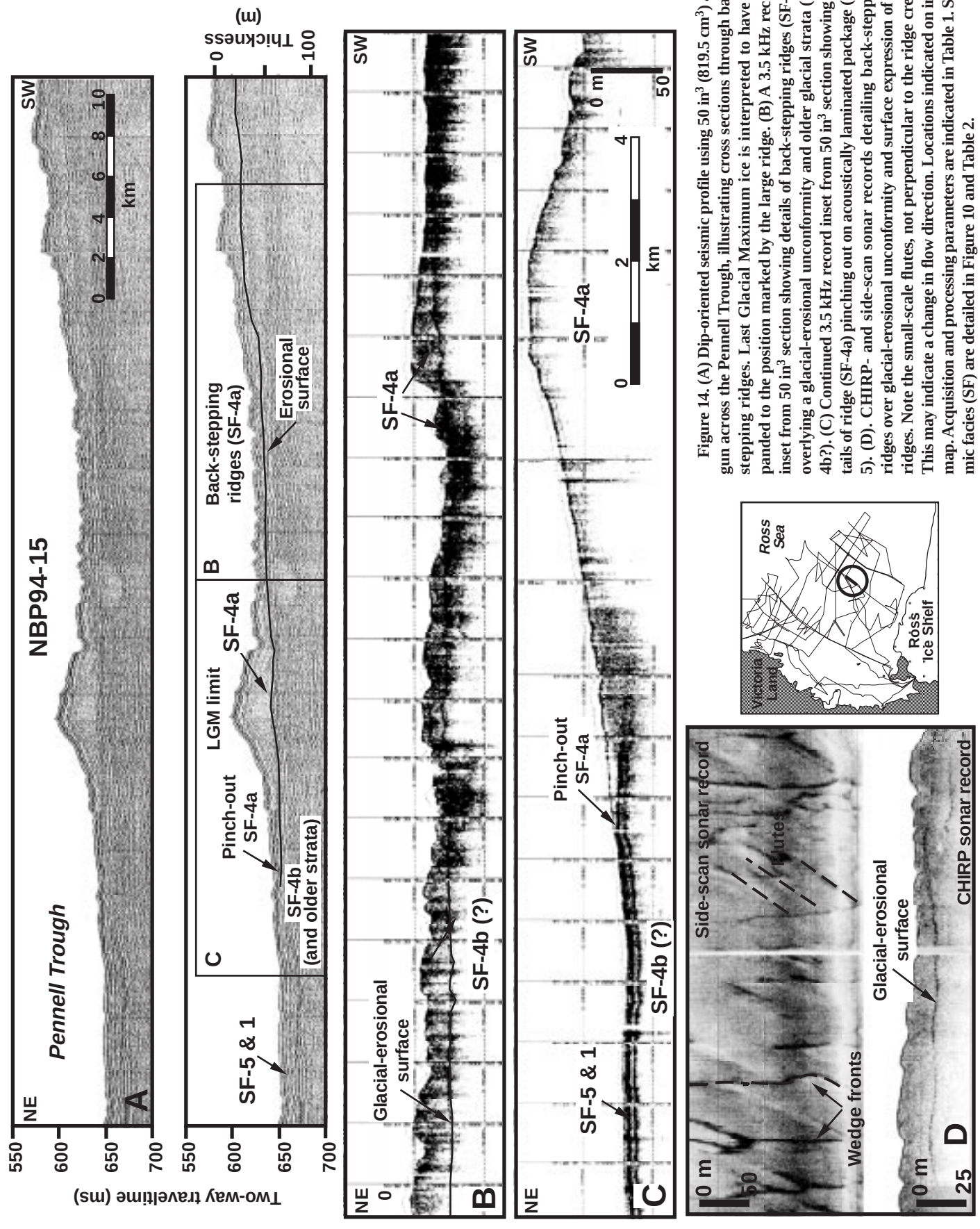

Figure 14. (A) Dip-oriented seismic profile using 50 in^3 (819.5 cm^3) air-gun across the Pennell Trough, illustrating cross sections through back-stepping ridges. Last Glacial Maximum ice is interpreted to have expanded to the position marked by the large ridge. (B) A 3.5 kHz record inset from 50 in^3 section showing details of back-stepping ridges (SF-4a) overlying a glacial-erosional unconformity and older glacial strata (SF-4b?). (C) Continued 3.5 kHz record inset from 50 in^3 section showing details of ridge (SF-4a) pinching out on acoustically laminated package (SF-5). (D). CHIRP- and side-scan sonar records detailing back-stepping ridges over glacial-erosional unconformity and surface expression of the ridges. Note the small-scale flutes, not perpendicular to the ridge crests. This may indicate a change in flow direction. Locations indicated on inset map. Acquisition and processing parameters are indicated in Table 1. Seismic facies (SF) are detailed in Figure 10 and Table 2.

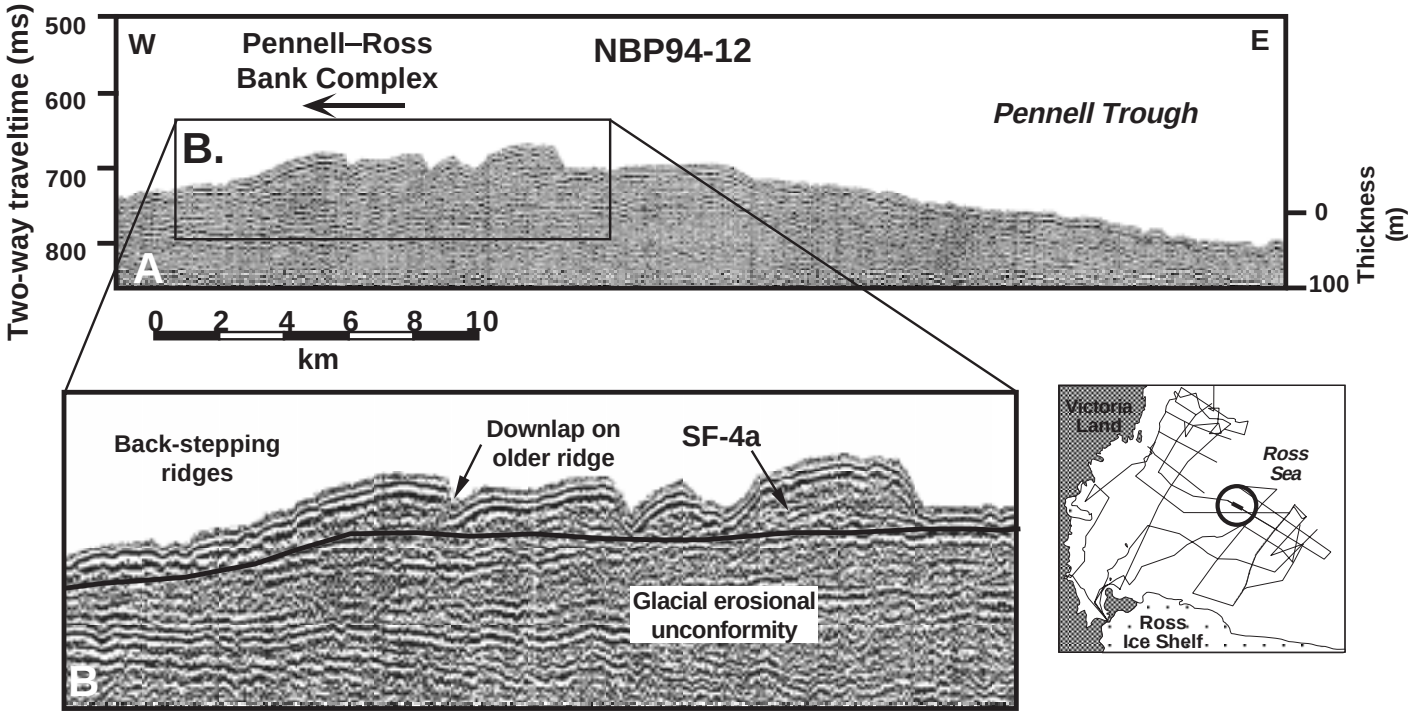

Figure 15. Dip-oriented seismic profile using 50 in^3 (819.5 cm^3) airgun over ridges on the Pennell Bank flank. Ice is interpreted to have been grounded on the bank top and retreated to the west in a step-like fashion. Locations indicated on inset map. Acquisition and processing parameters are indicated in Table 1. Seismic facies (SF) are detailed in Figure 10 and Table 2.

underscores a difference in the shelf setting of the ice sheets in the Ross Sea compared to those studied by King and Fader (1986) and King et al. (1991). The foredeepened nature of the Antarctic continental shelf precludes significant accommodation space, except at the shelf edge (where the shelf-edge moraine of pre-LGM, seismic facies 4b, deposits occurs) and the limited space available at the grounding line. Advance of the ice sheet cannibalized the "advance tills" excluding the seawardmost deposit. Retreat of the ice sheet in the Ross Sea across the foredeepened surface resulted in a landward shift in the grounding zone, leaving isolated wedges or till tongues of retreat till.

Mawson-Crary and Pennell-Iselin-Ross Banks. Thick wedges of seismic facies 4a occur on the bank flanks. These deposits occasionally display clinoforms that prograde into the adjacent trough (Fig. 4). The flanks may be draped by seismic facies 1. Thinner lenses of seismic facies 4a occur along the southern margin of Ross Bank. These deposits are fluted, with lineations wrapping around the bank. The bank tops of the Ross Sea contain patchy, thin deposits of seismic facies 4a in the southern regions; an erosional surface is exposed at the surface to the north. Abundant iceberg furrows occur on the bank flanks and tops, with larger furrows restricted to the landward regions and the flanks. Many of the seismic profiles crossing the bank tops record a gentle dip to the east and "steps" close to the bank edges, eroded into the older, flat-lying strata.

Sediment distribution, geomorphic features, and bank morphology are interpreted to indicate that the banks played a significant role in the glacial history of the region. The banks deflected ice flow, as suggested by the bidirectionality of the mega-scale glacial lineations in the sediment on the southern side of Ross Bank (Fig. 6). The maximum extent of ice on Mawson-Crary banks is placed north of the Coulman Island grounding-zone wedge to the west. This is supported by the shift from a patchy, thin deposit of seismic facies 4a to an exposed older surface seaward and the presence of downlapping wedges of material from the flanks into the Victoria Land Basin trough. Grounded ice on the Pennell-Iselin banks also is interpreted to have expanded beyond the Coulman Island grounding-zone wedge, on the basis of attached flank wedges and a marked step eroded into the bank top. Ice flow was divergent on the top of banks, but may have had a net flow to the west, resulting in increased erosion in the east, as indicated by the gentle eastward-dipping gradient of the bank tops. Embayments in the grounding line, perhaps covered by ice shelves attached to the bank edges, occurred in the troughs. Ice remained on the bank tops after retreat from the troughs, on the basis of the presence of back-stepping ridges of seismic facies 4a on the eastern flank of the Pennell-Iselin banks (Figs. 14 and 15) and on the downlap of attached flank wedges onto the surface of seismic facies 3 on the western side of the Pennell-Iselin banks (Fig. 4).

Pennell Trough. Four seismic facies are observed in the Pennell Trough (Figs. 11 and 14). The associations are similar to those found in the JOIDES Basin. Seismic facies 4a forms a series of linear ridges on the flank of the Pennell Bank, resting on a relatively smooth erosional surface (Fig. 14). Side-scan sonar images show that smaller ridges are organized in a similar manner (Fig. 14D). The ridges are younger toward the bank top and downlap onto seismic facies 5, which, in turn, drapes seismic facies 4b (Fig. 14, B and C). Facies 4b may crop out at the continental-shelf edge. Seismic facies 1 drapes facies 4a and 5. No facies similar to 2 or 3 is observed.

The base of the Pennell Trough is interpreted to have remained free of

grounded ice during the last glacial expansion across Ross Sea. Seismic facies 4b is interpreted to be associated with a previous glacial expansion, on the basis of similar associations in JOIDES Basin; a radiocarbon chronology does not exist for this region. Facies 5, interpreted to contain sub–ice-shelf and open-marine deposits, may include sediment from the previous interglacial time.

The large ridges observed on the flank of the Pennell Bank, rimming the Pennell Trough, are interpreted to be ice-edge moraines that formed as the grounded ice retreated from the trough and across the bank following the LGM (Figs. 14, A and B, and 15). Each ridge marks a retreat and pause of the grounding line. Ice flowed perpendicular to the ridge trend, as indicated by the orientation of the ridges and the presence of faint lineations. Barnes (1987) observed similar 50-m-high asymmetric ridges with the gentle gradient dipping into the troughs on the edge of Mertz Bank off Wilkes Land and suggested that the steep side of the features faced an ice margin. He interpreted the features as lateral ridges (possibly moraines) deposited as the ice from Mertz and Ninnis glaciers advanced and diverged around Mertz Bank (Barnes, 1987; Eittreim et al., 1995). In this study, the steep side of the moraine is interpreted as being away from the ice; the age relationship observed in the stepped moraines indicates that the ridges formed in association with retreating bank-top ice, rather than waning trough ice.

During the LGM and subsequent retreat, an ice shelf may have been present seaward of the Pennell Bank ridges. Again, this configuration would be similar to that proposed for JOIDES Basin. The grounding zone perhaps formed an embayment in the trough, with the ice shelf grounded on the adjacent highs. The acoustically laminated deposits of seismic facies 5 would include the resultant sub–ice-shelf deposits.

Central Ross Sea. Intratrough sheet deposits of seismic facies 4a characterize the strata interpreted to be associated with the last glacial expansion in the central Ross Sea (Figs. 11 and 13, A and B). A lack of higher-resolution data precludes further division; piston and kasten cores sampled diatomaceous mud of seismic facies 1. Two sheets resting on and downlapping onto a common flat, erosional unconformity occur on the middle to outer shelf. These show affinities with single till tongues of King and Fader (1996) and King et al. (1991). Deposition appears to reflect the influence of two sediment transport paths within the trough; the deposits show a depocenter associated with the deeper parts of the trough on the inner shelf. The outer shelf deposits show thinner accumulations along the continuation of the transport paths. Patchy, thin (<5 m) deposits of facies 4a occur on the innermost shelf (Fig. 11). In addition, bedrock drumlins occur on the inner shelf, and well-defined mega-scale glacial lineations occur seaward on the sheet deposit surface (Figs. 6 and 8). Both features indicate the presence of grounded ice in this region. The strata in the central Ross Sea are thicker and more extensive than in the western Ross Sea (Fig. 11). The contrast is attributed to differences in subglacial geology. Ice expanding into the western Ross Sea crossed seaward-dipping, lithified Miocene sedimentary strata (Hayes and Frakes, 1975). Ice advancing into the central Ross Sea passed over the Central trough and Eastern basin. These basins contain thick sequences of unconsolidated Pliocene–Pleistocene sedimentary strata (Hayes and Frakes, 1975). Hence, more unconsolidated sediment was available to the central Ross Sea glacial system.

Thrust faults cut the shelf-edge sheet deposits, and a system of gullies occurs at the slope break (Fig. 13, B and C). These features are interpreted to result from grounded ice at the continental-shelf break. The low-angle thrust faults are interpreted to represent shortening associated with a zone of compressive flow on the outer edges of the ice sheet (Fig. 13B; Bluemle and Clayton, 1984; Croot, 1987; van der Wateren, 1995). Ice overran the thrust sheets, as indicated by the presence of mega-scale glacial lineations on the surface. The gullies tentatively are interpreted to have been carved by turbidity currents initiated at the grounding line of the extended ice sheet (Figs. 6 and 13C). As the turbidity currents flowed down slope, they cut channels that coalesced and then diverged where the gradient decreases, depositing the sediment load in a slope fan. The gullies occur in proximity to the faults and may reflect additional input of meltwater evacuated from the detachment zones (e.g., Croot, 1987). Similar features are observed on other glaciated margins. Carlson et al. (1990) observed gullies at the shelf edge and on the upper slope of the Gulf of Alaska. They interpreted the features to result from sediment-gravity flows associated with postglacial storm and tide reworking of shelf-edge moraines. Depths in the Ross Sea are below storm reworking. Features of similar scale also were observed by Vorren et al. (1989). Because the gullies they identified are not filled with sediment, Vorren et al. (1989) suggested they are interglacial features, serving as conduits for winter downslope transport of cold, dense shelf water. The Ross Sea shelf break is a zone of active current scour. If the gullies were active during the last glaciation and ceased to be active during interglacial periods, they may not be infilled by sediment.

Distribution of facies 4a deposits may reflect two stages of glaciation: expansion to the outer shelf and retreat followed by a pause and renewed deposition of a middle shelf grounding-zone deposit. Alternatively, the LGM ice sheet may have advanced only to the middle shelf; the outer shelf deposits could be associated with a previous glaciation. An absolute chronology is needed to determine which scenario is correct.

DISCUSSION

Most high-latitude margins experience temperate phases of deglaciation during which thick glacial-marine sequences are deposited from large quantities of meltwater production (e.g., Anderson and Ashley, 1991; Josenhans and Zevenhuizen, 1990; King et al., 1991; Syvitski et al., 1996). Glacial-marine deposits often obscure images of small-scale features produced subglacially and make direct sampling of subglacial materials difficult. The Ross Sea continental shelf offers an opportunity to gain insight into the processes of deglaciation in a polar-marine setting. The features and deposits described above are used to develop possible scenarios for (1) LGM extent and thickness in the Ross Sea; (2) configuration of the ice-sheet system (e.g., paleo-glacial drainage, presence of ice streams) and conditions at the base of the ice sheet; and (3) relative deglacial history in the Ross Sea. The incorporation of radiocarbon chronologies adds constraints to the timing of events (Domack et al., 1999a; Licht et al., 1995, 1996; Cunningham et al., 1999). Figure 16 summarizes the proposed events in the deglaciation of the present Ross Sea continental shelf.

Maximum Extent and Thickness of Ice During the Last Glacial Minimum

Mega-scale glacial lineations define the limit of grounded ice, negating the minimum reconstructions of Drewry (1979) and Stuiver et al. (1981). The proposed reconstruction fits well with Denton et al.'s (1989) maximum reconstruction for the Ross Sea, in which they hypothesized extensive grounded ice without active ice streams.

JOIDES–Central and Victoria Land–Drygalski Basins. The LGM grounding-line position of ice in the western Ross Sea troughs of JOIDES-Central and Victoria Land–Drygalski basins is interpreted to be marked by the seismically and sedimentologically identified grounding-zone wedges and associated glacial-marine deposits on the outer shelf (Figs. 12 and 16A; Anderson et al., 1992; Domack et al., 1995a, 1999a; Licht, 1995; Licht et al., 1995, 1996, 1999; Shipp and Anderson, 1995; Shipp et al., 1995; Hilfinger et al., 1995), by mega-scale glacial lineations and other streamlined features, and by the presence of laminated deposits seaward of the grounding zone (Figs. 6 and 11). Using Hughes's (1995) equation for

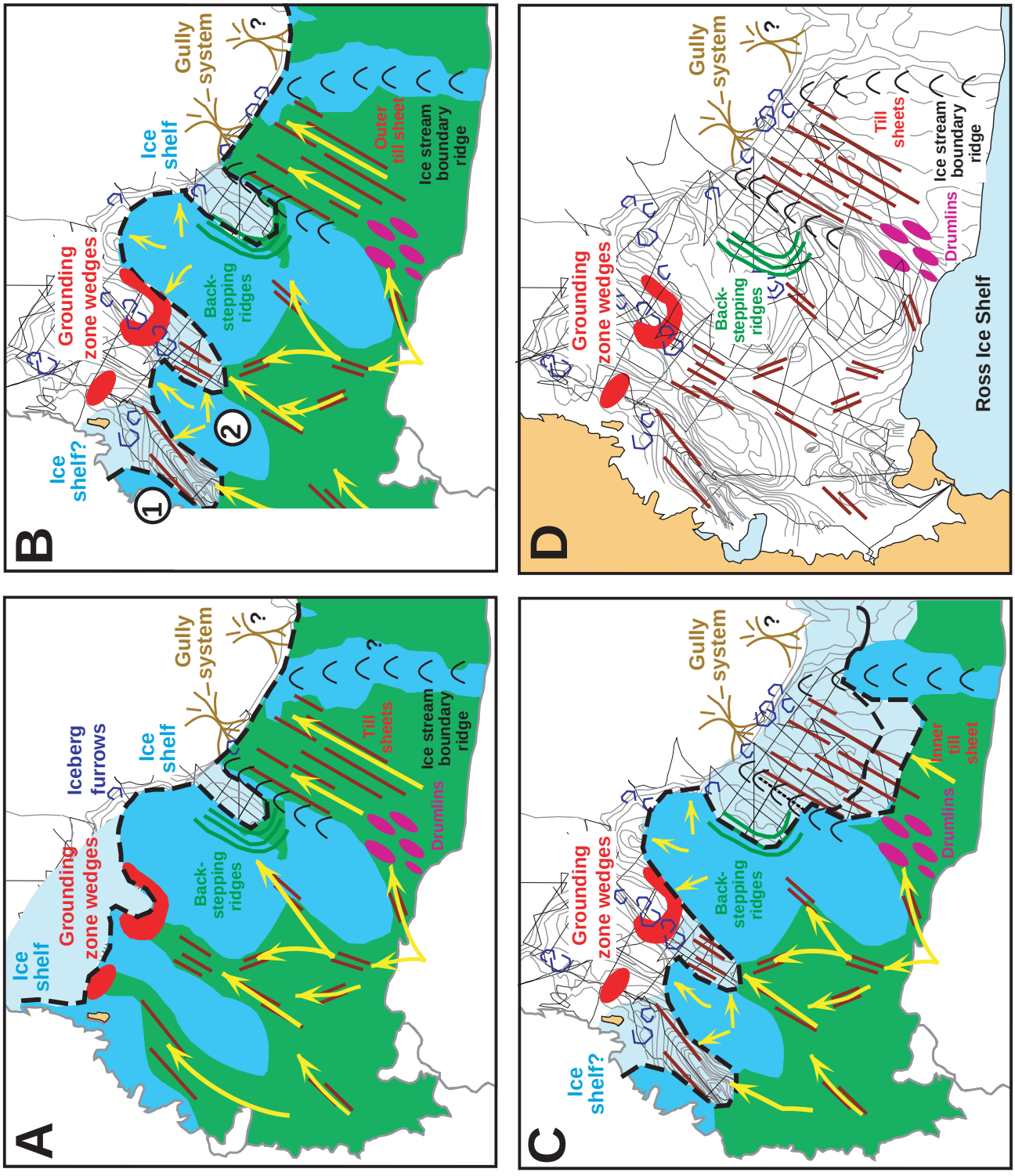

Figure 16. Summary diagram of proposed events in the deglaciation of the present Ross Sea continental shelf. (A) Maximum extent. Grounding-zone wedges are deposited on the continental shelf of the western Ross Sea and in the Pennell Trough; a till sheet is deposited across the central Ross Sea. Gully systems are active where the ice is at the continental-shelf edge. (B) Initial retreat phase from the western Ross Sea. Ice is interpreted to have evacuated the Victoria Land Basin first (marked by a 1) and subsequently retreated from the JOIDES Basin (marked by a 2). Off-bank deposits are not shown. (C) Continued retreat of the ice sheet, with ice receding from the central Ross Sea. No additional grounding-zone features are observed on the continental shelf of the western or central Ross Sea, interpreted to indicate a relatively rapid retreat. Ice remained on the bank tops, depositing sediment as flank-attached wedges in vacated troughs and in retreating bank-flank ridge systems (not shown). (D) Present continental-shelf setting with location of features.

calculating thickness of the ice margin at the grounding line of a marine-based ice sheet, the ice had a minimum thickness of 635 m:

$$h_{ice} = h_{water} (\rho_{seawater}/\rho_{ice}), \quad (1)$$

where h = height; ρ = density; h_{water} = 554 m; $\rho_{seawater}$ = 1030 kg/m^3; and ρ_{ice} = 900 kg/m^3.

In the western Ross Sea, the grounding-zone wedge and associated glacial-marine deposits observed in the JOIDES Basin constrain the maximum extent to 150 km south of the continental-shelf break, approximately 90 km north of the grounding zone defined by Licht et al. (1999). The extension results from the observation that the surface of the glacial-marine deposits is fluted; the ice sheet overrode the proglacial deposits of Licht et al. (1996, 1999). Deformation of the subglacial materials was minimal; radiocarbon stratigraphies are preserved intact. Radiocarbon stratigraphies support the LGM reconstruction (Domack et al., 1995a, 1999a; Licht, 1995; Licht et al., 1995, 1996, 1999; Hilfinger et al., 1995).

In Victoria Land Basin, the grounding zone tentatively is placed north of Coulman Island, ~130 km inland of the continental-shelf break and 110 km north of the grounding line set by Licht et al. (1996, 1999). Seismic records indicate that the trough contains thick deposits interpreted to be till; determination of subunits is problematic because of poor data quality. Licht et al. (1996, 1999) placed the LGM grounding line between two zones: (1) a zone south of the grounding line in which deposits are interpreted to be subglacial diamictons and exhibit younger (LGM) ages in the material immediately overlying the till; and (2) a zone north of their proposed grounding line, in which the deposits have a glacial-marine signature and contain older dates. Licht et al.'s (1999) grounding line is placed centrally within a core data gap of ~100 km. Eltanin core 52-8 occurs at the northern limit of the core data gap. This core was determined to contain subglacial material in earlier investigations, based on a uniform petrographic signature and lack of stratification (e.g., Anderson et al., 1992). Licht et al.(1996, 1999) considered Eltanin core 52-8 to contain glacial-marine diamicton, and presented a magnetic susceptibility record of consistent values. If the core contains subglacial material, this moves the Licht et al. (1999) grounding line ~50 km north of their proposed position. In addition, the cores used by Licht et al. (1996) contain a hiatus from the critical time span of approximately 20 k.y. B.P. to early Holocene (interpreted to represent presence of an ice shelf). Large furrows occur in the vicinity of many of the outer shelf cores; iceberg plowing may have removed the sediment. The placement of the grounding zone in this study may be too far north, based on the presence of interpreted tephra layers close to Coulman Island (Licht et al., 1999). However, the location of the grounding zone presented in this work is constrained by new data that reveal the presence of mega-scale glacial lineations north of Licht et al.'s (1999) grounding line. The lineations may indicate overriding of proximal glacial-marine–proglacial deposits by the ice sheet, similar to interpreted events in the JOIDES Basin. North of the proposed grounding line the deposits are characterized by a ponded seismic signature and may represent deposits of seismic facies 5. The western Ross Sea configuration fits reasonably well with Denton et al.'s (1989) model and with Kellogg et al.'s (1996) 16 k.y. B.P. reconstruction. Kellogg et al. (1996) indicated that their 16 k.y. B.P. reconstruction could be the maximum. Their placement of the LGM extent to the shelf edge is based on the foredeepened nature of the sea floor beyond Coulman Island; foredeepening could have resulted from prior glaciation.

Pennell Trough and Central Ross Sea. Ice in the Pennell Trough is interpreted to have grounded on the bank flanks, but not in the outer portion of the trough. Fluted grounding-zone ridges ring the trough. Acoustically laminated deposits occur seaward of the ridges; the upper surface shows no ice-contact influence. Using a water depth of 536 m at the seawardmost grounding zone, ice was at least 615 m thick in this region.

In the central Ross Sea the ice sheet is interpreted to have reached close to the continental-shelf edge during the LGM (Figs. 13 and 16A). At depths in excess of 550 m, the sea floor is sculpted into mega-scale glacial lineations and drumlins, formed under the expanded ice sheet (Figs. 6 and 16A). Shallower areas are iceberg scoured and contain no record of preexisting mega-scale glacial lineations. Faults that offset glacial strata are interpreted to be glacial-tectonic features (thrusts), thus supporting an ice sheet expanded close to the shelf edge (Fig. 13). The shelf-edge gullies are interpreted to be associated with turbidity flows initiated at the extended ice-sheet edge (Figs. 6 and 13). Based on Hughes's (1995) equation for marine ice margin thickness, the ice was at least 660 m thick at the grounding line in the central Ross Sea (where h_{water} = 576 m).

Denton et al.'s (1989) maximum reconstruction in the central Ross Sea showed ice grounded at the continental-shelf edge, with the exception of a small region on the outer central Ross Sea continental shelf. The extensive till sheets, mega-scale glacial lineations, glacial-tectonic features, and shelf-edge gullies support the Denton et al. (1989) model. Only the Pennell Trough remained ice-free; seismic data record acoustically laminated strata, which may be sub–ice-shelf to open marine in origin (Fig. 16A). The Pennell Trough embayment was not reflected in the Denton et al. (1989) model. Like the Pennell Trough, timing of deposition in the central Ross Sea is lacking. The outer shelf deposits could be associated with an earlier glaciation or glaciations (thus supporting Denton et al.'s (1989) minimum model). However, preliminary radiocarbon dates support the presence of ice grounded across the continental shelf during the LGM (Licht and Andrews, 1997; Domack et al., 1999a).

Configuration and Basal Conditions of the Ice Sheet

Paleo-Glacial Drainage and Presence of Ice Streams. Mega-scale glacial lineations and other geomorphic features provide an indicator of paleo-glacial drainage at the ice-sheet base (Fig. 6). On the inner shelf, lineations close to the banks indicate divergence of ice flow around the banks into the troughs. An accumulation of sediment occurs on the southern margin of the Ross-Pennell bank complex. Within the troughs, the lineations parallel the trough trend. On the central Ross Sea outer shelf, the lineations diverge slightly in the main trough, following the two sub-troughs. Ice is interpreted to have flowed around the banks in the Ross Sea, depositing a wedge of sediment where it met resistance and converged into the troughs. On the Pennell Bank, faint lineations occur perpendicular to the bank edge, between the back-stepping grounding-zone ridges. Flank-attached wedges and lenses, exhibiting clinoforms building in the direction of the troughs, occur in association with bank edges in the western Ross Sea (Fig. 4). Thinner ice, flowing in divergent directions, is interpreted to have occupied the banks. This ice transported material off the banks, depositing it at the ice margin on the bank flanks, a process that continued during ice retreat from the troughs (Fig. 15).

Ice streams are interpreted to have occupied regions of convergent ice flow in the troughs of the continental shelf during at least the late stages of the maximum ice advance. Slower moving, divergent ice is hypothesized to have occupied the banks between paleo-ice streams. The trough and ridge bathymetry of the Ross Sea floor is similar to the bathymetry at, and in front of, the present grounding-line setting of ice streams and intra–ice-stream regions; this bathymetry may reflect prior expansion of the ice streams across the continental shelf (Hughes, 1977). Present-day ice streams occupy regions of convergent ice flow and move at accelerated rates compared to the adjacent portions of the ice sheet (e.g., Bentley, 1987; Shabtaie et al., 1987). Mega-scale glacial lineations on the inner shelf indicate that a component of ice flow diverged at the landward bank edges and flowed into the troughs. Thus, expanded ice converged into the

troughs on the present continental shelf and may have experienced accelerated stream flow.

The pattern of erosion and/or thin deposition observed on the inner shelf within the troughs is believed to reflect accentuated flow along the trough axes (Boulton, 1990; Shipp et al., 1994a, 1995; Eittreim et al., 1995). The ice streams are interpreted to have transported material from the inner shelf and conveyed it to the grounding zones on the middle and outer shelf (Fig. 11). In the western Ross Sea, inner shelf erosion was particularly pronounced. This may reflect repeated reoccupation of the troughs by streaming ice through several glacial cycles. Mega-scale glacial lineations record at least two directions of ice flow (Fig. 12A-I), although it is unclear at what time the lineations were created. The bidirectionality of lineations may reflect advance and retreat phases, or it may reflect different flow directions during different glaciations. The middle and outer-shelf sediment deposits in the western Ross Sea are not organized as a terminal moraine that is an extensive line of accumulated debris parallel to the ice front. Rather, the deposits are organized in discrete patches within individual troughs, indicating a point-source distribution in the trough axes. (Fig. 11; Bart et al., 1995).

Deposits associated with the LGM are thin on the bank tops as well as in the inner shelf troughs. Ice flow on the banks is interpreted to have been divergent, on the basis of the sparse lineations and on the presence of grounding-zone deposits rimming the flanks in some regions (Fig. 11). Material was transported away from the banks to the edges. The lack of grounding-zone ridges toward the center of the banks may reflect intense reworking by icebergs. Alternatively, the ice on the banks may have become stagnant in the later stages of deglaciation, and/or the thinner ice may have decoupled from the bank tops as sea level rose, leaving thin deposits.

In the central Ross Sea, the troughs are wider and the ridges separating streams are rounded with clinoforms that indicate a laterally accreting component to the ridges (Fig. 5). Shifting ice streams may have dominated the central Ross Sea system, with little, slow-moving ice. The clinoforms within the central and eastern Ross Sea ridges are interpreted as lateral accretion sets, reflecting lateral migration of the ice streams (Alonso et al., 1992; Anderson et al., 1992; Shipp and Anderson, 1994a, 1995). The Central High (Fig. 2) separated two ice streams; downstream of the bathymetric high the ice streams flowed together and deposited a ridge at their boundary (Fig. 5). Alternatively, the deposits may reflect lateral flow of ice and sediment from an ice stream when it extended beyond the adjacent ice stream. These features may not have been active during the LGM; a thin unit, interpreted to be associated with the LGM, lies on the surface of the ridges. The age of the ridges is undetermined. However, distinct ridges similar in scale and configuration occur in association with each of the upper two seismic stratigraphic units interpreted by Alonso et al. (1992) to be Pleistocene in age, indicating that the ridges were constructed in a single glacial cycle.

Petrographic analyses provide additional support for distinct paths of ice flow. Sediment samples from individual troughs reveal distinct mineralogic signatures, corroborating the theory of distinct flow paths of ice within the troughs (Fig. 1; e.g., Anderson et al., 1980, 1984, 1992; Jahns, 1994). As the ice passes over the basement along the flow path, it incorporates a mineralogic signature of that source region. The sediment is carried along at the bed of the ice and eventually deposited at the base of the ice within the trough.

On the basis of the preceding observations, five lines of evidence support the presence of streaming ice on the continental shelf of the Ross Sea: (1) the existence of troughs; (2) the concentration of sedimentary deposits in the troughs on the central shelf; (3) the concentration of mega-scale glacial lineations within the trough axes; (4) the presence of central Ross Sea ridges displaying lateral accretion; and (5) the continuity of mineralogic provinces within the troughs. Denton et al. (1989) reasoned that active ice streams, such as exist today, would drain the ice sheet, thereby precluding a steepened ice-sheet profile and the attainment of a maximum configuration. Considered in total, the results of this investigation support streaming ice within the troughs. However, these attributes do not provide information about the relative or absolute rate of ice-stream flow or rate relative to ice flow on the bank tops, nor can the timing of onset of streaming ice be determined with the present data set.

Conditions at the Base of the Marine-Based Ice Sheet. The expanded ice sheet is interpreted to have been actively flowing within the troughs over a deforming substrate. The data do not support the presence of "free" meltwater.

The presence of drumlins indicates active, locally extensional glacier flow in association with basement highs (Aylsworth and Shilts, 1989; Lundqvist, 1989); these features occur in a trough for which streaming ice has been proposed (Fig. 8). The drumlins also may be linked to the presence of more easily eroded material (Aylsworth and Shilts, 1989) and the resultant increased rate of ice flow at the transition in substrate type from basement to sedimentary strata. The relative roles of water, ice, erosion, and deposition in the formation of the drumlins cannot be determined from the present data set, nor can the distance at which the drumlins formed inside the ice margin. Formation of drumlins may lead to irregularities at the base of the ice that serve as cavities for lineation formation as the ice advances, hence the observed transition from drumlins to mega-scale glacial lineations.

The presence of surficial mega-scale glacial lineations has been invoked to indicate a deforming substrate (e.g., Menzies, 1989; C. Clark, 1993, 1994; P. Clark, 1994). The Ross Sea floor exhibits mega-scale glacial lineations at the sediment-water interface within the troughs (Figs. 6 and 7). The surface underlying the massive, fluted unit is flat where observed. It is hypothesized that the ice and the substrate moved at different rates resulting in the creation of flutes (Fig. 7) and hummocks (Fig. 10B) in the sediment surface. Mobile till is interpreted to have carved the lower erosional surface.

The paucity of meltwater features is interpreted to support the deforming substrate model, although channels <1 m are not resolvable on the side-scan sonar data. Channeled meltwater is not likely to occur in regions of deforming substrate (Boulton and Hindmarsh, 1987; Alley et al., 1989; Clark and Walder, 1994). The mechanism of deforming substrate requires incorporation of meltwater into the substrate; channel forms cannot be maintained in the mobile material. Where the ice begins to float, close to the grounding line, the sediment strength diminishes, making channelization of meltwater possible (Boulton and Hindmarsh, 1987; Alley et al., 1989), hence channels might be expected close to the maximum ice positions in the Ross Sea if meltwater is present. No conclusive evidence of meltwater influence was observed in the data. The pore-water chemistry of the subglacial deposits yields a marine signature (Rayne and Domack, 1996). This supports the suggestion that little meltwater existed at the base of the ice sheet and that the ice sheet cannibalized preexisting glacial and glacial-marine sediment, and/or that deposition of the material was into the marine environment.

The subglacial deposits on the Ross Sea continental shelf are interpreted to have been emplaced by a mechanism similar to that proposed by Alley et al. (1989), and later modified by King (1993). Erosion rates along ice streams are high and require relatively rapid deposition at or near the grounding line. On the basis of seismic data, Blankenship et al. (1986) inferred a several-meter-thick layer of water-saturated deforming till at UpB camp of ice stream B. Subsequent investigation revealed a similar layer at DnB camp, almost 300 km farther down the ice stream. As the deforming till moves, it erodes the surface of the substrate below; Alley et al. (1989) reported furrows eroded into the surface of the underlying substrate. Ultimately the deforming till is deposited at the ice-stream terminus as a till "delta." Deposition in the marine environment would result in a sediment with an ice-proximal glacial-marine signature. The deposits prograde via a conveyer-belt recycling mechanism as the ice sheet advances over the top

of previously deposited material cannibalizing material from the more interior portions of the ice sheet (e.g., Powell, 1984; Alley et al., 1989).

On the Ross Sea continental shelf, the size and shape of the till delta is interpreted to be controlled predominantly by availability of sediment, accommodation space under and in front of the ice at the grounding zone, and duration of the grounding event. In the western Ross Sea, limited material is available for recycling; the grounding-zone wedge is relatively restricted in extent. In the central Ross Sea the upper seismic stratigraphic units are extensive wedges. The central and eastern Ross Sea are downstream of several basins containing thick unconsolidated and consolidated sedimentary strata that could be eroded by an advancing ice sheet. Little accommodation space was available under the ice sheet toward its terminal edge on the continental shelf. The wedges reflect the basal profile of the ice sheet to some extent, as indicated by the lineations on the landward slopes.

Deforming substrate could have initiated and accelerated the drainage of the ice sheet (Alley et al., 1987a, 1987b; Englehardt et al., 1990), resulting in thinning and eventual floatation of the ice sheet. MacAyeal (1992) modeled collapse of the West Antarctic Ice Sheet based on formation of a mobile bed. His findings indicate that substantial drainage of ice from the ice sheet could be facilitated by acceleration of ice-stream flow caused by a deforming substrate. Quasi-periodic collapse of the ice sheet could occur on the order of a few hundred years every hundred millennia (MacAyeal, 1992). Additional data are needed to evaluate this scenario, including information on alternative triggers for retreat of the expanded ice sheet, e.g., impinging warm-water masses or accumulated sea-level rise. Detailed radiocarbon stratigraphies are necessary to determine the rate of retreat and if the ice sheet was out of phase with other global phenomena. The results from this investigation indicate that the ice sheet was resting on a deforming bed in its outer reaches. Perhaps the deforming bed resulted in rapid flow and thinning of the expanded ice sheet, initiating retreat out of phase with other natural events.

Retreat History

Maximum. Alley et al. (1989) proposed that a several-meter-thick layer of unconsolidated sediment occurs at the mouth of ice stream B. It rests on a unit that is tens of meters thick and contains beds dipping downstream at approximately 0.5°. The feature, tens of kilometers long, is similar in external geometry and size to the isolated wedge in JOIDES Basin. Based on estimates of sediment flux to the grounding zone, Alley et al. (1989) suggested that the wedge could form in a 5–10 k.y. time span. Radiocarbon dates from the glacial-marine deposits overlying the subglacial deposits of the Coulman Island wedge yield uncorrected total organic carbon ages of ca. 14.290 ka (corrected value of 11.150 ka; see Domack et al., 1999a), marking the latest possible retreat from this position. Based on the Alley et al. (1989) estimates, the feature could have formed approximately 19–24 ka, corresponding to the LGM estimates of Hall and Denton (1998) and Licht and Andrews (1997). Flux rates would have been higher using the Alley et al. (1989) model, on the basis of the expanded region of erosion under the maximum ice sheet; the feature could have formed faster, making these estimates maxima. Timing of the maximum and initiation of retreat is less certain for the Pennell Trough and central Ross Sea regions. Ice is placed at the trough edge and the outer shelf break, respectively.

Break-Up. Large iceberg scours occur in association with grounding zones in water depths that exceed the theoretical depth of present-day iceberg keels (maximum of 500 m). This implies larger icebergs, formation during lower sea level, or a combination of the two. With a sea level 120 m lower, this places the greatest water depths in which the icebergs occur, 600 m, at 480 m; this value still is close to the theoretical maximum and does not take into account isostatic loading by the ice sheet. Thus, the scours are interpreted to indicate possible mass wasting of the ice sheet during the initial phase of deglaciation (Figs. 6 and 9) and imply the absence of an ice shelf, at least temporarily, during this break-up phase. The large icebergs became trapped behind the outer shelf banks. Rising sea level and disintegration of the icebergs eventually permitted their passage across the outer shelf; commonly the southern side of the banks are more iceberg-scoured than the surface.

Retreat. Ice within the troughs appears to have occurred independently, on the basis of differing radiocarbon histories in individual troughs (Domack et al., 1995b, 1999a; Hilfinger et al., 1995), and on the lateral changes recorded in the intertrough regions (Fig. 16B; Alonso et al., 1992; Anderson et al., 1992; Shipp and Anderson, 1994a, 1994b, 1995). The independent nature of the ice streams may be significant with respect to the deglaciation of the Ross Sea; it appears from the radiocarbon chronology that ice retreated along the Victoria Land Basin–Drygalski Trough first, followed by retreat from the JOIDES basin (Hilfinger et al., 1995; Domack et al., 1999a). Kellogg et al.'s (1996) reconstructions suggest a similar early retreat along the western margin of the ice sheet. Retreat from the western Ross Sea, in particular from the Victoria Land Basin–Drygalski Trough, may have initiated instability of the system. Much of the ice occupying the Victoria Land Basin–Drygalski Trough and JOIDES Basin–Central trough must flow from the East Antarctic Ice Sheet across the Transantarctic Mountains. The retreat of ice in these troughs may be linked to a diminished contribution from the East Antarctic Ice Sheet (Kellogg et al., 1996). The Victoria Land Basin–Drygalski Trough has the steepest landward-dipping gradient of all the shelf troughs; once retreat began, the foredeepened nature of the basin contributed to collapse (Hughes, 1987). Retreat of ice from the Victoria Land Basin–Drygalski Trough may have triggered thinning of ice in the adjacent troughs as ice flowed westward to fill the void, thus destabilizing the entire system and leading to disintegration of the expanded ice sheet. Lateral accretion and downlap of materials derived from Mawson Bank into Victoria Land Basin–Drygalski Trough suggests that grounded ice occurred on the banks and deposited material into a trough vacant of ice (Fig. 16B).

Ice retreated first from the troughs in the western Ross Sea (Domack et al., 1999a; Hilfinger et al., 1995), possibly resulting in a configuration of ice being grounded on the banks and floating over the troughs, depositing an ice-edge moraine at a grounding line that paralleled the trough (Fig. 16, B and C). This configuration may have created the wedges that downlap into the troughs, observed on some seismic strike lines. The ice-edge moraines on the eastern boundary of the Pennell Bank become younger toward the interior of the bank, suggesting that an extended, grounded ice mass remained on the bank and retreated in steps, depositing ice-edge moraines during pauses in retreat (Fig. 16C). Presence of acoustically laminated sediment seaward of the ridges supports the presence of an ice shelf, perhaps during the retreat phase, as well.

In the central Ross Sea, ice is inferred to have remained pinned to the outer shelf longer than in the western Ross Sea, primarily because of the shallower depth of the continental shelf (Fig. 16, B and C). During retreat, the ice paused on the central shelf, depositing an extensive till sheet prior to retreat landward of the present ice shelf (Fig. 16, C and D). This pause and associated deposition may reflect a greater availability of erodable substrate to the system and the more gentle shelf gradient.

In the western Ross Sea, subsequent retreat is predicted to have been relatively rapid in the foredeepened troughs; only the Coulman Island grounding zone is observed north of the present ice-shelf edge (Fig. 16, C and D). Significant pause in the troughs during retreat would have resulted in the deposition of additional grounding-zone features. Further constraints are drawn from work that indicates the ice margin passed Ross Island approximately 6.430 ± 0.070 ka (uncorrected; Denton et al., 1989, 1991; Licht et al., 1995), and from the sediment flux calculations

of Alley et al. (1989) that indicate the ice may have been at its present grounding position for 5–10 k.y. These data suggest grounded ice retreated from the Coulman Island region approximately 14 ka across a distance of almost 400 km to Ross Island by about 6.4 ka (a rate of ~50 m/yr) and retreated an additional 900 km in 1000 yr (6.430 ka minus the minimum 5000 yr estimate of Alley et al., 1989), yielding a rate of approximately 900 m/yr. The retreat rate calculated between the grounding zone at Coulman Island and Ross Island is not significantly different from the ice-shelf edge retreat rate of approximately 100 m/yr calculated by Domack et al. (1999a) for a site ~100 km south of Coulman Island to Granite Harbor. Both rates are similar to terrestrial ice-sheet margin retreat rates in the Northern Hemisphere for the LGM (Andrews, 1973; Dyke and Prest, 1987). The 900 m/yr is more extreme and exceeds calculations by Bindschadler (1997b) for the present-day ice sheet. If the retreat rate from Ross Island to the present-day grounding line is interpreted to have been essentially continuous since approximately 6400 yr B.P., the retreat rate would have been approximately 140 m/yr.

CONCLUSIONS

1. Based on identification of isolated grounding-zone wedges and consistency of mega-scale glacial lineations, the LGM grounded ice edge is interpreted to have extended to the Coulman Island region in the western Ross Sea. This interpretation correlates well with sedimentologic and radiocarbon stratigraphies (e.g., Domack et al., 1999a). Grounded ice was not present in the outer portion of the Pennell Trough. The maximum extent of grounded ice in central Ross Sea is placed at the continental-shelf edge, on the basis of the consistency of mega-scale glacial lineations, presence of glacio-tectonic features, and the existence of shelf-edge gullies. Although different in details, the proposed reconstruction agrees closely with the maximum reconstructions of Denton et al. (1989) and Licht et al. (1999) and with the 16 k.y. B.P. model of Kellogg et al. (1996) for the Ross Sea.

2. Streaming ice overlying a deforming bed is interpreted to have filled the troughs. Thinner, divergent, slower moving ice, not underlain by deforming sediment, is interpreted to have occupied the bank tops. Ice is interpreted to have transported material in a conveyor belt-like fashion. Materials were eroded from the ice-sheet interior and carried to the grounding zone, where they were deposited as an extensive grounding-zone wedge. During the expansion phase of the ice sheet, ice overrode and cannibalized the previous grounding-zone materials. Ice flowing into the central Ross Sea overrode sedimentary basins, resulting in thicker depositional packages and depositional ridges between expanded paleo-ice streams. Ice streams in the western Ross Sea did not tap a similar sedimentary source, therefore the sediment is thinner and the grounding zone is an isolated feature.

3. The shelf-wide presence of mega-scale glacial lineations and the paucity of meltwater features suggests that a deforming substrate beneath the ice streams may have been present and may have contributed to accelerated drainage of the West Antarctic Ice Sheet . Additional high-resolution radiocarbon stratigraphies are necessary to distinguish links between deglaciation and global events, e.g., sea-level rise, changes in ocean circulation.

4. The ice streams appear to have acted independently, on the basis of differing radiocarbon histories in individual ice streams (Domack et al., 1999a), and on the lateral changes recorded in the ice-stream boundaries. Ice retreated from the Victoria Land Basin–Drygalski Trough first, possibly because of a diminished contribution from the East Antarctic Ice Sheet, thus initiating instability of the expanded system. Ice remained on the outer shelf of the central Ross Sea after retreat began in the western Ross Sea. Retreating ice paused in the central Ross Sea, depositing a second grounding-zone feature. Ice remained grounded on the banks following ice retreat from the troughs, although ice shelves may have covered the trough regions. The bank ice may have become stagnant in the later stages of deglaciation and/or been floated off the banks rapidly, resulting in the absence of bank-top grounding-zone features.

5. The ice sheet may have undergone an initial phase of large-scale mass wasting, on the basis of the presence of large, arcuate iceberg furrows associated with the grounding zones in water depths too deep for scouring by the drafts of present-day icebergs.

6. Retreat of the ice sheet occurred throughout Holocene time and undoubtedly contributed to Holocene sea-level rise. The nature of this retreat may have been episodic (Bindschadler, 1998). The available data suggest that if a large-scale collapse of the ice sheet occurred, it took place later than ~6.4 ka when the grounding line retreated from a position near Ross Island to its present location. The marine geologic record of this sea-floor region is inaccessible because it is covered by the present ice shelf. Neither the geophysical data nor the radiocarbon chronologies (nor the global-eustatic sea-level curves) are sufficiently well constrained to speculate on meter-scale sea-level contributions.

ACKNOWLEDGMENTS

This research was funded by the National Science Foundation, Office of Polar Programs grants DPP-9119683 and OPP-9527876 to John Anderson. The authors extend their appreciation to the crew of the RV/IB *Nathaniel B. Palmer* and to the Antarctic Support Associates personnel for three pleasant and productive cruises. Marco Taviani, Fabio Trincardi, and Frederick Van der Wateren participated in data collection and offered many helpful ideas during the 1994 and 1995 cruises. Dale Chayes, Rob Haag, and Suzanne O'Hara of Lamont-Doherty Geological Observatory, Columbia University, and Michelle Fassell of Rice University, assisted in the processing of the 1995 multibeam data; Suzanne O'Hara participated in the processing of the 1998 data set. Gratitude also is extended to the Florida State University Antarctic Research Facility curatorial staff for their assistance in describing, sampling, and archiving of cores. Breezy Long patiently worked with the final figures for this manuscript. The research presented in this manuscript is part of a collaborative effort between researchers at Rice University, Hamilton College and the Institute of Arctic Alpine Research (INSTAAR) at the University of Colorado, Boulder. This work benefited greatly from discussions with Kathy Licht, Ross Powell, Philip Bart, and Julia Smith Wellner. Informal reviews by Kathy Licht and Jana DaSilva particularly have been helpful. The authors wish to thank reviewers John Andrews, Dan Belknap, Tom Kellogg, and Ralph Stea for their many helpful suggestions and comments.

REFERENCES CITED

Alley, R. B., Blankenship, D. D., Bentley, C. R., and Rooney, S. T., 1986, Deformation of till beneath ice stream B, West Antarctica: Nature, v. 322, p. 57–59.

Alley, R. B., Blankenship, D. D., Bentley, C. R., and Rooney, S. T., 1987a, Till beneath ice stream B 3. Till deformation: Evidence and implications: Journal of Geophysical Research, v. 92, p. 8921–8929.

Alley, R. B., Blankenship, D. D., Rooney, S. T., and Bentley, C. R., 1987b, Till beneath ice stream B 4. A coupled ice-till flow model: Journal of Geophysical Research, v. 92, p. 8931–8940.

Alley, R. B., Blankenship, D. D., Rooney, S. T., and Bentley, C. R., 1989, Sedimentation beneath ice shelves: The view from ice stream B: Marine Geology, v. 85, p. 101–120.

Alonso, B., Anderson, J. B., Diaz, J. T., and Bartek, L. R., 1992, Plio–Pleistocene seismic stratigraphy of the Ross Sea: Evidence for multiple ice sheet grounding episodes, *in* Elliot, D. H., ed., Contributions to Antarctic research III: Washington, D.C., American Geophysical Union, Antarctic Research Series, v. 57, p. 93–103.

Anderson, J. B., in press, Antarctic marine geology—Sedimentology: Cambridge, United Kingdom, Cambridge University Press.

Anderson, J. B., and Ashley, G. M., 1991, Glacial marine sedimentation, paleoclimatic significance: A discussion, *in* Anderson, J. B., and Ashley, G. M., eds., Glacial marine sedimentation, paleoclimatic significance: Geological Society of America Special Paper 261, p. 223–226.

Anderson, J. B., and Bartek, L. R., 1992, Ross Sea glacial history revealed by high resolution seismic reflection data combined with drill site information, *in* Kennett, J. P., and Warnke, D. A., eds., Antarctic research series, Volume 56: Washington, D.C., American Geophysical

Union, p. 231–263.
Anderson, J. B., and Thomas, M. A., 1991, Marine ice sheet decoupling as a mechanism for rapid, episodic sea-level change: The record of such events and their influence on sedimentation: Sedimentary Geology, v. 70, p. 87–104.
Anderson, J. B., Kurtz, D. D., Domack, E. W., and Balshaw, K. M., 1980, Glacial and glacial marine sediments of the Antarctic continental shelf: Journal of Geology, v. 88, p. 399–414.
Anderson, J. B., Brake, C. F., and Myers, N. C., 1984, Sedimentation in the Ross Sea, Antarctica: Marine Geology, v. 57, p. 295–333.
Anderson, J. B., Shipp, S. S., Bartek, L. R., and Reid, D. E., 1992, Evidence for a grounded ice sheet on the Ross Sea continental shelf during the late Pleistocene and paleodrainage reconstruction, *in* Elliot, D. H., ed., Contributions to Antarctic research III: Washington, D.C., American Geophysical Union Antarctic Research Series, v. 57, p. 39–62.
Andrews, J. T., 1973, The Wisconsin Laurentide ice sheet: Dispersal centers, problems of rates of retreat, and climatic implications: Arctic and Alpine Research, v. 5, p. 185–199.
Andrews, J. T., and Tedesco, K., 1992, Detrital carbonate-rich sediments, northwestern Labrador Sea: Implications for ice-sheet dynamics and iceberg rafting (Heinrich) events in the North Atlantic: Geology, v. 20, p. 1087–1090.
Attig, J. W., Mickelson, D. M., and Clayton, L., 1989, Late Wisconsin landform distribution and glacier bed conditions in Wisconsin: Sedimentary Geology, v. 62, p. 399–405.
Aylsworth, J. M., and Shilts, W. W., 1989, Bedforms of the Keewatin ice sheet, Canada: Sedimentary Geology, v. 62, p. 407–428.
Barnes, P. W., 1987, Morphologic studies of the Wilkes Land continental shelf, Antarctica—Glacial and iceberg effects, *in* Eittreim, S. L., and Hampton, M. A., eds., The Antarctic continental margin: Geology and geophysics of offshore Wilkes Land: Houston, Texas, Circum-Pacific Council for Energy and Mineral Resources, p. 175–194.
Barnes, P. W., and Lien, R., 1988, Icebergs rework shelf sediments to 500 m off Antarctica: Geology, v. 16, p. 1130–1133.
Bart, P. J., Trincardi, F., Shipp, S. S., and Anderson, J. B., 1995, Ice streams as sediment point sources for Plio–Quaternary deposition: Western Ross Sea: Siena, Italy, VII International Symposium on Antarctic Earth Sciences, p. 28.
Belknap, D. F., and Shipp, R. C., 1991, Seismic stratigraphy of glacial marine units Maine inner shelf, *in* Anderson, J. B., and Ashley, G. M., eds., Glacial marine sedimentation: Paleoclimatic significance: Geological Society of America Special Paper 261, p. 137–158.
Bentley, C. R., 1987, Antarctic ice streams: A review: Journal of Geophysical Research, v. 92, p. 8843–8858.
Bentley, C. R., 1997, Rapid sea-level rise soon from West Antarctic Ice Sheet collapse?: Science, v. 275, 1077–1078.
Bentley, C. R., and Jezek, K. C., 1981, RISS, RISP, and Riggs: Post-IGY glaciological investigations of the Ross Ice Shelf in the U.S. program: Journal of the Royal Society of New Zealand, v. 11, p. 355–372.
Bindschadler, R. A., 1997a, West Antarctic Ice Sheet collapse? Discussion: Science, v. 276, p. 662–664.
Bindschadler, R. A., 1997b, Actively surging West Antarctic ice streams and their response characteristics: Annals of Glaciology, v. 24, p. 409–414.
Bindschadler, R. A., 1998, Future of the West Antarctic Ice Sheet: Science, v. 282, p. 428–429.
Bindschadler, R .A., Alley, R. B., Anderson, J., Shipp, S., Borns, H., Fastook, J., Jacobs, S., Raymond, C. F., and Shuman, C. A., 1998, What is happening to the Antarctic Ice Sheet?: EOS (Transactions, American Geophysical Union), v. 79, p. 257, 264–265.
Blankenship, D. D., Bentley, C. R., Rooney, S. T., and Alley, R. B., 1986, Seismic measurements reveal a saturated porous layer beneath an active Antarctic ice stream: Nature, v. 322, p. 54–57.
Bluemle, J. P., and Clayton, L., 1984, Large-scale glacial thrusting and related processes in North Dakota: Boreas, v. 13, p. 279–299.
Bond, G., Heinrich, H., Broecker, W. S., Labeyrie, L., McManus, J., Andrews, J. T., Huon, S., Jantschik, R., Clasen, S., Simet, C., Tedesco, K., Klas, M., Bonani, G., and Ivy, S., 1992, Evidence for massive discharges of icebergs into the glacial northern Atlantic: Nature, v. 360, p. 245–249.
Boulton, G. S., 1990, Sedimentary and sea level changes during glacial cycles and their control on glacimarine facies architecture, *in* Scourse, J. A., and Dowdeswell, J. D., eds., Glacimarine environments: Processes and sediments: London, Geological Society Special Publication 53, p. 15–52.
Boulton, G. S., and Hindmarsh, R. C. A., 1987, Sediment deformation beneath glaciers: Rheology and geological consequences: Journal of Geophysical Research, v. 92, p. 9059–9082.
Boyce, J. I., and Eyles, N., 1991, Drumlins carved by deforming till streams below the Laurentide ice sheet: Geology, v. 19, p. 787–790.
Carlson, P. R., Bruns, T. R., and Fisher, M. A., 1990, Development of slope valleys in the glacimarine environment of a complex subduction zone, northern Gulf of Alaska, *in* Dowdeswell, J. A., and Scourse, J. D., eds., Glacimarine environments: Processes and sediments: London, Geological Society Special Publication 53, p. 139–153.
Clark, C. D., 1993, Mega-scale glacial lineations and cross-cutting ice-flow landforms: Earth Science Processes and Landforms, v. 18, p. 1–29.
Clark, C. D., 1994, Large-scale ice-moulding: A discussion of genesis and glaciological significance: Sedimentary Geology, v. 91, p. 253–268.
Clark, P. U., 1994, Unstable behavior of the Laurentide ice sheet over deforming sediment and its implications for climate change: Quaternary Research, v. 41, p. 19–25.
Clark, P. U., and Walder, J. S., 1994, Subglacial drainage, eskers, and deforming beds beneath the Laurentide and Eurasian ice sheets: Geological Society of America Bulletin, v. 106, p. 304–314.
Croot, D. G., 1987, Glacio-tectonic structures: A mesoscale model of thin-skinned thrust sheets?: Journal of Structural Geology, v. 9, p. 797–808.
Cunningham, W. L., Leventer, A., Andrews, J., Jennings, A., and Licht, K., 1999, Late Pleistocene–Holocene marine conditions in the Ross Sea, Antarctica: Evidence from the diatom record: The Holocene, p. 129–139.
Davey, F. J., 1994, Bathymetry and gravity of the Ross Sea, Antarctica: Terra Antarctica, v. 1, p. 357–358.
Debenham, F., 1921, Recent and local deposits of McMurdo Sound region: British Museum, Natural History Report, British Antarctic Expedition, Geology, v. 1, p. 63–90.
Denton, G. H., Bockheim, J. G., Wilson, S. C., and Stuiver, M., 1989, Late Wisconsin and early Holocene glacial history, inner Ross Embayment, Antarctica: Quaternary Research, v. 3, p. 151–182.
Denton, G. H., Prentice, M. L., and Burckle, L. H., 1991, Cainozoic history of the Antarctic Ice Sheet, *in* Tingey, R. J., ed., The geology of Antarctica: Oxford, United Kingdom, Clarendon Press, p. 365–433.
Domack, E. W., Hilfinger, M., Franceschini, J., Licht, K., Jennings, A., Andrews, J., Shipp, S., and Anderson, J. B., 1995a, New stratigraphic evidence from the Ross Sea continental shelf for instability of the West Antarctic Ice Sheet during the last glacial maximum: St. Pete Beach, Florida, SEPM (Society for Sedimentary Geology), First Congress on Sedimentary Geology, p. 46–47.
Domack, E. W., Hilfinger, M., and Franceschini, J., 1995b, Stratigraphic and facies relationships in the Ross Sea related to late Pleistocene fluctuation of the West Antarctic Ice Sheet system: Arlington, Virginia, West Antarctic Ice Sheet Initiative, Third Annual Science Workshop, p. 12.
Domack, E. W., Jacobson, E. K., Shipp, S., and Anderson, J. B., 1999a, Late Pleistocene–Holocene retreat of the West Antarctic Ice Sheet System in the Ross Sea: Part 2—Sedimentologic and stratigraphic signature: Geological Society of America Bulletin, v. 111, p. 1517–1536.
Domack, E. W., Taviani, M., Rodriguez, A., 1999b, Recent sediment remolding on a deep shelf, Ross Sea: Implications for radiocarbon dating of Antarctic marine sediments: Quaternary Geochronology (in press).
Drewry, D. J., 1979, Late Wisconsin reconstruction for the Ross Sea region, Antarctica: Journal of Glaciology, v. 24, p. 231–244.
Dyke, A. S., and Prest, V. K., 1987, Late Wisconsinan and Holocene history of the Laurentide ice sheet: Geographie Physique et Quaternaire, v. 16, p. 237–263.
Eittreim, S. L., Cooper, A. K., and Wannesson, J., 1995, Seismic stratigraphic evidence of ice sheet advances on the Wilkes Land margin of Antarctica: Sedimentary Geology, v. 96, p. 131–156.
Englehardt, H., Humphrey, N., Kamb, B., and Fahnestock, M., 1990, Physical conditions at the base of a fast moving Antarctic ice stream: Science, v. 248, p. 57–59.
Fairbanks, R., G., 1989, A 17 000-year glacio-eustatic sea level record: Influence of glacial melting rates on the Younger Dryas event and deep ocean circulation: Nature, v. 342, p. 637–642.
Franceschini, J. 1995, Preservation of total organic carbon in sediments from the Ross Sea, Antarctica [B.A. thesis]: Hamilton, New York, Hamilton College, 98 p.
Hall, B. L., and Denton, G. H., 1998, Deglacial chronology of the Western Ross Sea from terrestrial data: Orono, Maine, American Geophysical Union, Chapman Conference, Scientific Program and Abstracts, West Antarctic Ice Sheet, 13–18 September, p. 27–28.
Hayes, D. E., and Davey, F. J., 1975, A geophysical study of the Ross Sea, Antarctica, *in* Hayes, D. E., and Frakes, L., eds., Initial reports of the Deep Sea Drilling Project, Volume 28: Washington, D.C., U.S. Government Printing Office, p. 887–907.
Hayes, D. E., and Frakes, L., 1975, General synthesis, Deep Sea Drilling Project Leg 28, *in* Hayes, D. E., and Frakes, L., eds., Initial reports of the Deep Sea Drilling Project, Volume 28: Washington, D.C., U.S. Government Printing Office, p. 919–941.
Heinrich, H., 1988, Origin and consequences of cyclic ice rafting in the northeast Atlantic Ocean during the past 130 000 years: Quaternary Research, v. 29, p. 143–152.
Hilfinger, M., Franceschini, J., and Domack, E. W., 1995, Chronology of glacial marine lithofacies related to the recession of the West Antarctic Ice Sheet in the Ross Sea: Antarctic Journal of the United States, 1995 Review Issue, v. 30, p. 82–84.
Hollin, J. T., 1962, Origin of ice ages: An ice shelf theory for Pleistocene glaciation: Nature, v. 202, p. 1099–1100.
Houtz, R., and Davey, F. J., 1973, Seismic profiler and sonobuoy measurements in Ross Sea, Antarctica: Journal of Geophysical Research, v. 78, p. 3448–3468.
Hughes, T., 1973, Is the West Antarctic Ice Sheet disintegrating?: Journal of Geophysical Research, v. 78, p. 7884–7910.
Hughes, T. J., 1977, West Antarctic ice streams: Reviews of Geophysics and Space Physics, v. 15, p. 1–46.
Hughes, T. J., 1987, Deluge II and the continent of doom: Rising sea level and collapsing Antarctic ice: Boreas, v. 16, p. 89–99.
Hughes, T. J., 1995, Ice sheet modeling and the reconstruction of former ice sheets from glacial geo(morpho)logical field data, *in* Menzies, J., ed., Modern glacial environments: Processes, dynamics, and sediments. Glacial Environments Volume 1: Oxford, United Kingdom, Butterworth and Heinemann, p. 77–99.
Jacobs, S. S., Helmer, H. H., and Jenkins, A., 1996, Antarctic Ice Sheet melting in the southeast Pacific: Geophysical Research Letters, v. 23, p. 957–960.
Jahns, E., 1994, Evidence for a fluidized till deposit on the Ross Sea continental shelf: Antarctic Journal of the United States, 1994 Review Issue, v. 29, p. 139–141.
Jenkins, A., Vaughan, D. G., Jacobs, S. S., Hellmer, H. H., and Keys, J. R., 1996, Glaciological and oceanographic evidence of high melt rates beneath Pine Island Glacier, West Antarctica: Journal of Glaciology, v. 43, p. 114–121.
Jennings, A. E., Xiao, J., Licht, K. J., and Andrews, J. T., 1995, Benthic foraminiferal assemblages from the western Ross Sea: Approximately 30 000 years ago to present: Antarctic Journal of the United States, 1995 Review Issue, v. 30, p. 26–28.
Johnson, G. L., Vanney, J. R., and Hayes, P., 1982, The Antarctic continental shelf: A review, *in* Craddock, C., ed., Antarctic geosciences: Madison, University of Wisconsin Press, p. 22–27.
Josenhans, H. W., and Zevenhuizen, J., 1990, Dynamics of the Laurentide ice sheet in Hudson Bay, Canada: Marine Geology, v. 92, p. 1–26.

Karl, H. A., Reimnitz, E., and Edwards, B. D., 1987, Extent and nature of Ross Sea unconformity in the western Ross Sea, Antarctica, *in* Cooper, A. K., and Davey, F. J., eds., The Antarctic continental margin. Earth Science Series, Volume 5B: Geology and Geophysics of the Western Ross Sea: Houston, Texas, Circum-Pacific Council for Energy and Mineral Resources, p. 77–92.

Kellogg, T. B., Hughes, T., and Kellogg, D. E., 1996, Late Pleistocene interactions of East and West Antarctic ice-flow regimes: Evidence from the McMurdo Ice Shelf: Journal of Glaciology, v. 42, p. 486–499.

King, L. H., 1993, Till in the marine environment: Journal of Quaternary Science, v. 8, p. 347–358.

King, L. H., and Fader, G. B. J., 1986, Wisconsinan glaciation of the Atlantic continental shelf of southeast Canada: Geological Survey of Canada Bulletin 363, 72 p.

King, L. H., Rokoengen, K., Fader, G. B. J., and Gunleiksrud, T., 1991, Till-tongue stratigraphy: Geological Society of America Bulletin, v. 103, p. 637–659.

Lewis, J. C., and Bennett, G., 1984, Monte Carlo calculations of iceberg draft changes caused by roll: Cold Regions Science and Technology, v. 10, p. 1–10.

Licht, K. J., 1995, Marine sedimentary record of ice extent and late Wisconsin deglaciation in the Western Ross Sea, Antarctica [Master's thesis]: Boulder, University of Colorado, 144 p.

Licht, K. J., and Andrews, J. T., 1997, Central Ross Sea deglaciation estimates from 21 new radiocarbon dates: Sterling, Virginia, Agenda and Abstracts, Fourth Annual Workshop, West Antarctic Ice Sheet Initiative, 10–13 September.

Licht, K. J., Hilfinger, M. F., Franceschini, J. M., Domack, E. W., Jennings, A. E., and Andrews, J. T., 1995, New marine stratigraphic evidence for glaciation across the Ross Sea continental shelf: Ice sheet or ice shelf?: International Symposium on Antarctic Earth Sciences, 7th, Siena, Italy, p. 244.

Licht, K. J., Jennings, A. E., Andrews, J. T., and Williams, K. M, 1996, Chronology of late Wisconsin ice retreat from the western Ross Sea, Antarctica: Geology, v. 24, p. 223–226.

Licht, K. J., Dunbar, N. W., Andrews, J. T., and Jennings, A. E., 1999, Distinguishing subglacial till and glacial marine diamictons in the western Ross Sea, Antarctica: Implications for last glacial maximum grounding line: Geological Society of America Bulletin, v. 111, p. 91–103.

Lingle, C. S., and Clark, J. A., 1979, Antarctic Ice-Sheet volume at 18 000 years B.P., and Holocene sea level changes at the West Antarctic margin: Journal of Glaciology, v. 24, p. 213–230.

Lingle, C. S., Schilling, D. H., Fastook, J. L., Paterson, W. S. B., and Brown, T. J., 1991, A flow band model of the Ross Ice Shelf, Antarctica: Response to CO_2-induced climatic warming: Journal of Geophysical Research, v. 96, p. 6849–6871.

Lundqvist, J., 1989, Glacigenic processes, deposits, and landforms, *in* Goldthwait, R. P., and Matsch, C. L., eds., Genetic classification of glacigenic deposits: Rotterdam, Netherlands, Balkema, p. 3–16.

MacAyeal, D. R., 1992, Irregular oscillations of the West Antarctic Ice Sheet: Nature, v. 359, p. 29–32.

McCann, S. B., and Kostaschuk, R. A., 1987, Fjord sedimentation northern British Columbia, *in* Fitzgerald, D. M., and Rosen, P. S., eds., Glaciated coasts: New York, Academic Press, p. 33–49.

Menzies, J., 1989, Subglacial hydraulic conditions and their possible impact upon subglacial bed formation: Sedimentary Geology, v. 62, p. 125–150.

Oppenheimer, M., 1998, Global warming and the stability of the West Antarctic Ice Sheet: Nature, v. 393, p. 325–332.

Orheim, O., 1980, Physical characteristics and life-expectancy of tabular Antarctic icebergs: Annals of Glaciology, v. 1, p. 11–18.

Potter, J. R., and Paren, J. G., 1985, Interactions between ice shelf and ocean in George VI Sound, Antarctica, *in* Jacobs, S. S., ed., Oceanology of the Antarctic continental shelf: Washington, D.C., American Geophysical Union, Antarctic Research Series, v. 43, p. 35–58.

Powell, R. D., 1984, Glacimarine processes and inductive lithofacies modeling of ice shelf and tidewater glacier sediments based on Quaternary examples: Marine Geology, v. 57, p. 1–52.

Pudsey, C. J., Barker, P. F., and Larter, R. D., 1994, Ice sheet retreat from the Antarctic Peninsula shelf: Continental Shelf Research, v. 14, p. 1647–1675.

Rayne, T., and Domack, E. W., 1996, Pore water geochemistry of Ross Sea diamictons: A till or not a till?: Antarctic Journal of the United States, v. 31, p. 97–98.

Reid, D. E, 1989, Late Cenozoic glacial-marine, carbonate, and turbidite sedimentation in the northwestern Ross Sea, Antarctica [Master's thesis]: Houston, Texas, Rice University, 178 p.

Shabtaie, S., Whillans, I. M., and Bentley, C. R., 1987, The morphology of ice streams A, B, and C, West Antarctica, and their environs: Journal of Geophysical Research, v. 92, p. 8865–8883.

Shipp, S., and Anderson, J. B., 1994a, High-resolution seismic survey of the Ross Sea continental shelf: Implications for ice-sheet retreat behavior: Antarctic Journal of the United States, 1994 Review Issue, v. 29, p. 137–138.

Shipp, S., and Anderson, J. B., 1994b, Late Pleistocene deglaciation of Ross Sea Antarctica inferred from high-resolution seismic data: Geological Society of America Abstracts with Programs, v. 26, no. 7, p. 364.

Shipp, S., and Anderson, J. B., 1995, Late Quaternary deglacial history of Ross Sea, Antarctica: Results from recent seismic investigation: International Symposium on Antarctic Earth Sciences, 7th, Siena, Italy, p. 347.

Shipp, S., Anderson, J. B., and Domack, E. W., 1995, Images of the last glacial maximum, Ross Sea, Antarctica: Geological Society of America Abstracts with Programs, v. 27, no. 6, p. 61–62.

Solheim, A., Russwurm, L., Elverhoi, A., and Berg, M. N., 1990, Glacial geomorphic features in the northern Barents Sea: Direct evidence for grounded ice and implications for the pattern of deglaciation and late glacial sedimentation, *in* Dowdeswell, J. A., and Scourse, J. D., Glacimarine environments: Processes and sediments: London, Geological Society, Special Publication 53, p. 253–268.

Stuiver, M., Denton, G. H., Hughes, T. J., and Fastook, J. L., 1981, History of the marine ice sheet in West Antarctica during the last glaciation: A working hypothesis, *in* Denton, G. H., and Hughes, T. J., eds., The last great ice sheets: New York, Wiley, p. 319–439.

Sugden, D. E., and John, B., 1976, Glaciers and landscapes, landforms of glacial deposition: London, Edward Arnold, p. 235–257.

Syvitski, J. P. M., Andrews, J. T., and Dowdeswell, J. A., 1996, Sediment deposition in an iceberg-dominated glacimarine environment, East Greenland: Basin fill implications: Global and Planetary Change, v. 12, p. 251–270.

ten Brink, U. S., Schneider, C., and Johnson, A. H., 1995, Morphology and stratal geometry of the Antarctic continental shelf: Insights from models, *in* Cooper, A. K., and Davey, F. J., eds., The Antarctic continental margin, Earth Science Series, Volume 5B: Geology and Geophysics of the Western Ross Sea: Houston, Texas, Circum-Pacific Council for Energy and Mineral Resources, p. 1–24.

Thomas, M. A., and Anderson, J. B., 1994, Sea-level controls on the facies architecture of the Trinity/Sabine incised-valley system, Texas Continental Shelf: SEPM (Society for Sedimentary Geology) Special Publication 51, p. 63–82.

Thomas, R. H., and Bentley, C. R., 1978, A model for Holocene retreat of the West Antarctic Ice Sheet: Quaternary Research, v. 10, p. 150–170.

Van der Wateren, F. M., 1995, Processes of glaciotectonism, *in* Menzies, J., ed., Modern glacial environments. Glacial environments, Volume 1: Oxford, United Kingdom, Butterworth-Heinemann, p. 309–335.

Vorren, T. O., Lebesbye, E., Andreassen, K., and Larsen, K.-B., 1989, Glacigenic sediments on a passive margin as exemplified by the Barents Sea: Marine Geology, v. 85, p. 251–272.

MANUSCRIPT RECEIVED BY THE SOCIETY DECEMBER 2, 1997
REVISED MANUSCRIPT RECEIVED NOVEMBER 12, 1998
MANUSCRIPT ACCEPTED DECEMBER 15, 1998

Printed in U.S.A.